CHALMERS

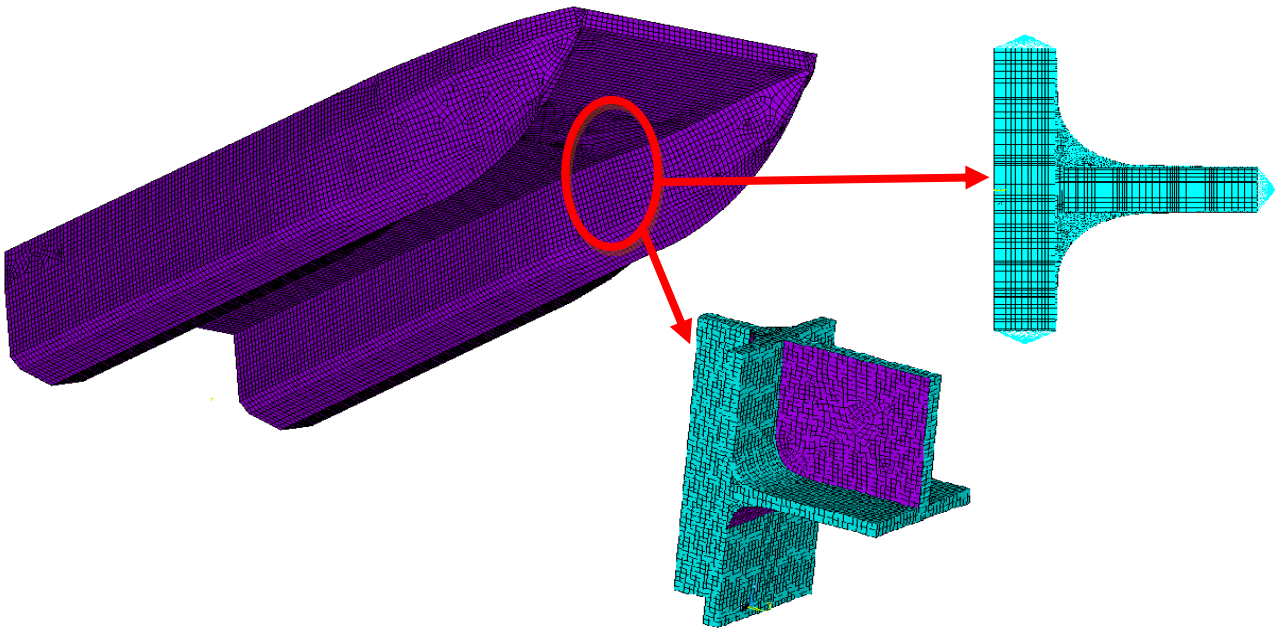

# Parametric Study of Joint Design in a HSLC Composite Vessel – Load-carrying Characteristics of Foam Core and Joint Geometry in Sandwich Structures

*Master of Science Thesis*

CHRISTIAN NÄSLUND
OSMAN OZAN UYANIK

Department of Shipping and Marine Technology
*Division of Ship Design*
CHALMERS UNIVERSITY OF TECHNOLOGY
Gothenburg, Sweden, 2011
Report No. X-11/257

A THESIS FOR THE DEGREE OF MASTER OF SCIENCE

# Parametric study of joint design in a HSLC composite vessel – Load-carrying characteristics of foam core and joint geometry in sandwich structures

CHRISTIAN NÄSLUND
OSMAN OZAN UYANIK


Department of Shipping and Marine Technology
CHALMERS UNIVERSITY OF TECHNOLOGY
Gothenburg, Sweden 2011

Parametric study of joint design in a HSLC composite vessel –
load-carrying characteristics of foam core and joint geometry in sandwich structures

CHRISTIAN NÄSLUND
OSMAN OZAN UYANIK



Report No. X-11/257

Department of Shipping and Marine Technology
Chalmers University of Technology
SE-412 96 Gothenburg
Sweden
Telephone +46 (0)31-772 1000

Printed by Chalmers Reproservice
Gothenburg, Sweden, 2011

Parametric study of joint design in a HSLC composite vessel –
load-carrying characteristics of foam core and joint geometry in sandwich structures

CHRISTIAN NÄSLUND
OSMAN OZAN UYANIK

Department of Shipping and Marine Technology
Division of Ship Design
Chalmers University of Technology

## Abstract

Composite sandwich ships have laminated joints that contribute to a significant part of the ship's weight. Their construction requires an extensive amount of man-hours. There is great potential for weight and production-time reduction through alternative joint designs.

According to class rules, one is not allowed to benefit from the load-carrying capability of the core, i.e. the strength characteristics of the core shall be disregarded and geometry at joint locations is also disregarded. The objective of the current investigation was to investigate the possibility of constructing a joint were the load-carrying capability of the foam core is accounted for, leading to a reduction in weight and production time.

One specific joint in a 23 m composite sandwich catamaran was selected for study, a side wall-wet deck T-joint. This joint is considered as being crucial for the structural integrity of the current vessel. A global finite element (FE) model of the catamaran was designed and analysed in ANSYS. The loads and boundary conditions were applied to the global model according to DNV's HSLC rules. Two local FE models of the joints (2D and 3D) were utilized for a parametric analysis with respect to structure response (stress concentrations and compliance with failure and fracture criteria). Finally, the results and conclusions from the study show the possibilities and advantages of incorporating the foam core material as a load-carrying member in joint design without compromising safety.

*Keywords:* composite, core material, finite element, joint design, light weight, parametric analysis.

## Preface

This thesis is a part of the requirements for the Master's degree at Chalmers University of Technology, Gothenburg, and has been carried out at the Division of Ship Design, Department of Shipping and Marine Technology, Chalmers University of Technology and in collaboration with Kockums AB.

We would like to acknowledge and thank our examiner and supervisor, Professor Jonas Ringsberg at the Department of Shipping and Marine Technology for his contributions and valuable guidance throughout this work. We would also like to thank our co-supervisor, Luis Felipe Sánchez Heres, who first introduced us to composite sandwich modelling techniques and always guided us in all stages of the thesis. His remarkable effort contributed greatly to this thesis. We would also like to thank our supervisor Måns Håkansson from Kockums AB, who introduced us to the concept and provided us with necessary material. Finally, we would like to thank our classmates for the time spent together and for their contribution to us in all aspects.

Gothenburg, June, 2011
Christian Näslund & Osman Ozan Uyanık

# Contents

# Notations and abbreviations

## Symbols

| | |
|---|---|
| $E_f$ | Modulus of elasticity of face laminate [MPa] |
| $E_c$ | Modulus of elasticity of core [MPa] |
| $M_x$ | Moment around x-axis [Nmm] |
| $t_f$ | Thickness of a face laminate [mm] |
| d | Distance between neutral axis of two face laminates [mm] |
| D | Total flexural rigidity of sandwich [MPa] |
| $D_f$ | Flexural rigidity of laminates according to own neutral axis [MPa] |
| $D_o$ | Flexural rigidity of laminates according to sandwich neutral axis [MPa] |
| $D_c$ | Flexural rigidity of core according to sandwich neutral axis [MPa] |
| $\sigma_f$ | Normal stress of the laminate [MPa] |
| $\sigma_c$ | Normal stress of the core [MPa] |
| $T_x$ | Shear force [N] |
| $\tau_x$ | Shear stress [MPa] |

## Abbreviations

| | |
|---|---|
| DNV | Det Norske Veritas |
| FE | Finite element |
| HSLC | High-speed light craft |
| LÄSS | Lightweight construction applications at sea |
| LWL | Waterline length |
| PVC | Polyvinyl chloride |

# 1. Introduction

## 1.1. Background

Composite sandwich materials have, during the last few years, gained importance as construction materials in shipbuilding. The Kockums shipyard in Sweden has developed the lightweight catamaran CarboCAT seen in Fig. 1, a class of vessels ranging from 18-43 m with an application as passenger vessels and wind farm support vessels. Another shipyard emerging within lightweight shipbuilding is the Norwegian shipyard Brødrene Aa that specialises in passenger transport catamarans up to 40 m. The Swedish joint research project Lightweight Construction Applications at Sea (LÄSS) concluded that the construction with composite sandwich materials could also be beneficial for other applications, such as ferry superstructures and cargo vessel deck houses [1]. The main benefit of using these materials is that a lower structural weight is achieved while strength and stiffness are maintained compared to using conventional materials such as steel and aluminium. Reduced weight results in an improved payload to fuel consumption ratio, which has positive effects on both the environment and on ship operator economy. An additional benefit of composite sandwich materials is that the production methods offer the possibility of efficiently manufacturing complex structural shapes.

**Fig. 1.** Kockums CarboCAT 23 CarboClyde.

The idea of the sandwich concept is the utilization of stiff face sheets which are separated by a low-density core material. The face sheets carry axial load and bending moment, while the core carries shear load and provides support against buckling and wrinkling of the faces. The importance of joints in sandwich structures is stressed by Kildegaard [2] who mentions that 2 km of joint can be found on a typical 50 m sandwich ship and that they contain 10% of the structural weight. The joints between sandwich panels are critical to the overall structural integrity because a discontinuity between the laminates arises. Due to this, the normal load has to be carried by the core material, which is much weaker than the laminates. The challenge is described more thoroughly in Chapter 2.3.

Generally, there are two ways of dealing with the discontinuity: to add an external fillet structure with overlaminates that distributes the load over a larger cross section of core material or to construct a joint with continuity between the laminates. The latter solution is more complicated from a production point of view. Classification rules [3] do not allow a load to be carried by the core material and also do not account for the load distribution from fillet structures without special consideration. Thus, there is a desire to gain more knowledge on joints that carry a load with the core material.

The theory of the behaviour of sandwich structures has been well established, and, among others, Zenkert [4] presents a good overview. Steeves and Fleck [5] successfully predicted failure of composite sandwich beams with a PVC core in 3-point-bending tests by means of analytical expressions as well as FE-analysis. It was concluded from their experiments that for typical sandwich configurations core material yielding is the first type of failure. Most previous studies on joints have focused on joint tensile strength. Lystrup and Toftegaard [6] made an investigation on the improvement of T-joints for naval ships that concluded with a new triangular fillet joint specially optimised for tensile loads. Shenoi and Violette [7] made experiments testing the strength of T-joints loaded in compression. In the study, a joint with a small overlaminate radius (10 mm) came out as the most efficient regarding strength, weight and cost. Berggren et al. [8] conducted a computational and experimental analysis to improve the performance of X-joints (connection point of deck, superstructure and bulkhead) under compression loading in naval vessels. In this study, the authors emphasised the importance of core material selection and the geometry of the fillet structure.

In this thesis, a Kockums CarboCAT 23 CarboClyde [9] catamaran structure is used for obtaining realistic load conditions for a T-joint. A typical T-joint design utilised by Kockums is studied parametrically under these load conditions. CarboClyde is a new generation 23 m catamaran specially designed for wind farm support purposes with a displacement of 60 metric tonnes. The beam of the vessel is 8.8 m with a draft of 1.1 m. The ship is constructed with a sandwich structure made out of carbon fibre laminates impregnated with vinylester resin and Divinycell foams as core material. This vessel is the result of a unique combination of high-tech and lightweight ship production. However, the intention is to achieve a general approach and knowledge rather than dealing only with the design of the joints of the concerned vessel.

## 1.2. Objective

The objective of this thesis is to study the load-carrying capabilities of the core material and joint geometry in a typical composite sandwich T-joint design. The focus is on compressive loading of the core material and an investigation of the structural response of a proposed joint arrangement on a ship is used for demonstrating the potential of overlaminated joints. At the same time, it is desirable to gain a general knowledge of the stress-distributing effect of the joint geometry. The aim is to find relations between geometrical and material parameters and load-carrying capability. These parametric studies are aimed at improving the design of the investigated joint and to provide a basis for joint design guidelines. Moreover, while conducting 2D and 3D submodelling of the joints, the aim is to compare the feasibility of these two modelling techniques for this specific type of joint.

## 1.3. General description of methodology

In order to study the load-carrying capability of the joint, the worst loading condition for the joint of interest was needed. To find out this condition, global strength analyses of different loading conditions from the DNV High Speed Light Craft classification notes [10] were conducted. A global model was created in Rhinoceros 4.0 [11] and was converted into a shell finite element (FE) model and analysed in ANSYS 12.1 [12]. The global strength analyses revealed the worst condition that can occur in the joint of interest. This is the starting point of a safe and reliable joint design.

A submodelling technique was employed for detailed analyses of the specific areas of interest. Boundary conditions were extracted from the global analysis for application in a local 2D analysis. As well as 2D analysis, 3D parametric analyses were conducted in order to provide

sufficient knowledge about the load distribution in 3D. Finally, the results of the analyses were compiled into simple guidelines for joint design, focusing on joint geometry and material selection. In Fig. 2, a flow chart showing the general work procedure can be seen.

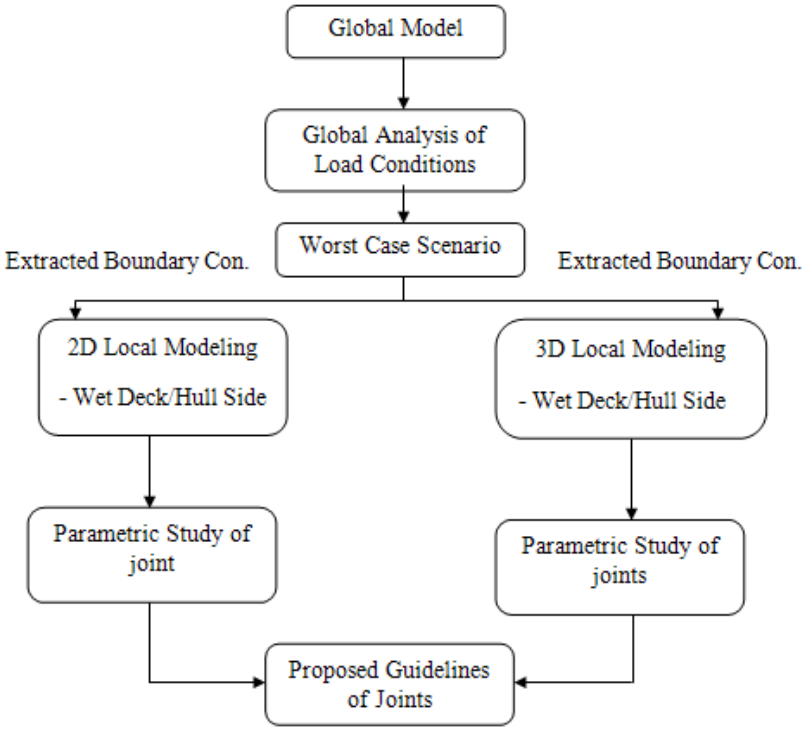


**Fig. 2.** Flow chart of the general work procedure.

## 1.4. Limitations and assumptions

The thesis is limited to investigating laminates made from carbon fibre/vinylester and Divinycell foam core materials. All materials are assumed to behave in a linear elastic manner in the models. The global model is made from shell elements, which means that the structure is treated as a thin-walled structure with wall stiffness equivalent to the stiffness of sandwich panels.

Only the basic structural members are included in the global model. The structure is therefore weaker than the real structure and should give conservative results. The applied load cases are in accordance with the DNV High Speed Light Craft classification notes, which take into account the fact that the real ship load conditions are dynamic rather than static.

Material imperfections, degradation and fatigue are left out of the study. Instead, safety factors are used to account for the negative effects of these. Finally, it is out of the scope of this thesis to conduct a weight and cost analysis of the joints.

# 2. Sandwich concept

## 2.1. Sandwich plates

Sandwich structures have a high flexural rigidity and low weight ratios compared to conventional structures composed of steel or aluminium. The high flexural rigidity is achieved via a high section modulus. High section modulus and low weight are the result of inserting low density core material between two stiff laminates.

As can be seen in Fig. 3, the main advantage of this concept is a substantial weight/stiffness ratio compared to other structure types and materials such as steel and aluminium. A benefit of using composite sandwich plates in a structure is that the amount of stiffeners can be reduced compared to similar structures in steel or aluminium, which leads to less complex structures, and, therefore, less points where fatigue damage may occur. However, there will still be a need for connecting two sandwich panels. These connections can be (in marine applications) for example; a bulkhead-hull side or a deck-hull side connection. These locations should be investigated thoroughly.

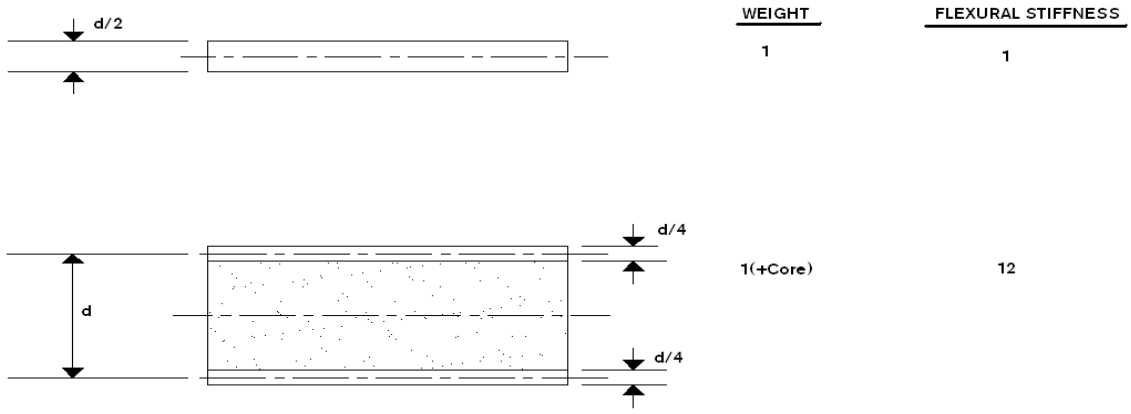


**Fig. 3.** Single laminate and sandwich structures compared in terms of flexural stiffness.

## 2.2. Fundamental equations for a sandwich structure

To have a better understanding of the sandwich concept and the stress distribution at the joints, it is wise to present the basic equations of sandwich beam theory; see Fig. 4 for a definition of cross-section loads, external loads and a definition of variables of a sandwich beam.

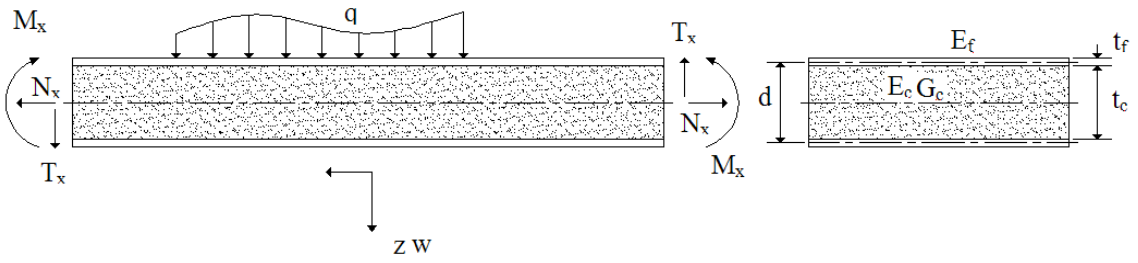


**Fig. 4.** Sign convention for sandwich beams.

The flexural stiffness of the sandwich beam can be expressed as:

$$D = \int Ez^2 dz = \frac{E_f t_f{}^3}{6} + \frac{E_f t_f d^2}{2} + \frac{E_c t_c{}^3}{12} = 2D_f + D_0 + D_c \tag{1}$$

The first two terms are the flexural stiffness of the laminates and last term is the stiffness of the core. Under the conditions of $t_f \langle\langle t_c$ and $E_c \langle\langle E_f$, the first two terms can be ignored. From Hooke's law, stresses due to bending can be achieved as:

$$\sigma_f = \frac{M_x z E_f}{D} \; for \; \frac{t_c}{2} \langle |z| \langle \frac{t_c}{2} + t_f \tag{2}$$

$$\sigma_c = \frac{M_x z E_c}{D} \; for \; |z| \langle \frac{t_c}{2} + t_f \tag{3}$$

If it is assumed that faces are thin and that the core is weak, the stresses can be expressed as:

$$\sigma_f = \pm \frac{M_x}{t_f d} \tag{4}$$

$$\sigma_c \approx 0 \tag{5}$$

Shear stresses of the beam can be expressed with assumptions and approximations, Zenkert[4] as:

$$\tau_f \approx 0 \tag{6}$$

$$\tau_c = \pm \frac{T_x}{d} \tag{7}$$

As can be seen from the simplified equations, the core carries the shear forces through the thickness of the beam and does not carry any normal forces. The face laminates carry the normal forces alone and do not carry any shear forces.

## 2.3. Sandwich joints

The main challenge of the sandwich connections is the discontinuity of the laminate because the in-plane reactions of one panel will affect the other panel through the thickness direction, see Fig. 5. Under these circumstances, Zenkert [1] mentions that the condition stating that the laminate face sheets carry all the normal forces will be violated.

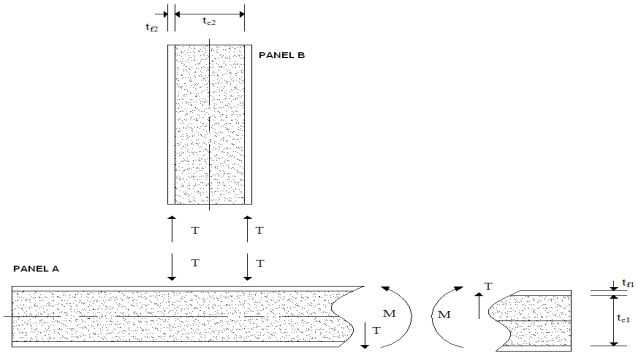


**Fig. 5.** Forces and moments in the joints.

The core shear stress at Panel A is:

$$\tau_c = \pm \frac{T}{t_{c1}} \tag{8}$$

The normal stress of the core through thickness at Panel A, is (see Fig. 5 for notations):

$$\sigma_c = \pm \frac{T}{t_{f2}} \tag{9}$$

Not only will the shear stress at the core of Panel A be a crucial point to observe, but also the through-thickness normal stresses in the core. This is due to stress concentrations that arise because the loads are transferred mainly via the face laminates of Panel B. Usually, foam core materials are more susceptible to compressive stresses than tensile stresses. For these reasons, compressive and shear failures of the core at Panel A are likely to occur. Thus, the distribution of load is an important issue.

Figure 6 shows a typical T-joint design that is utilised by Kockums. It is designed to minimise the problem of stress concentrations in the core material. A structural adhesive is placed between the panels. It is much weaker than the laminates and therefore deforms and distributes loads over a larger area. Fillet radii are built up between the panels with high density core material. On top of these fillets sheets of laminate are laid, so-called overlaminates. This added structure, which in this thesis will be referred to as joint geometry, helps distributing loads in the joint acting as two brackets. This is a lightweight design since the fillet radii are made of lightweight materials. The common practice by Kockums is to use structural adhesives to build up the fillet radii for smaller radii, typically r < 45 mm.

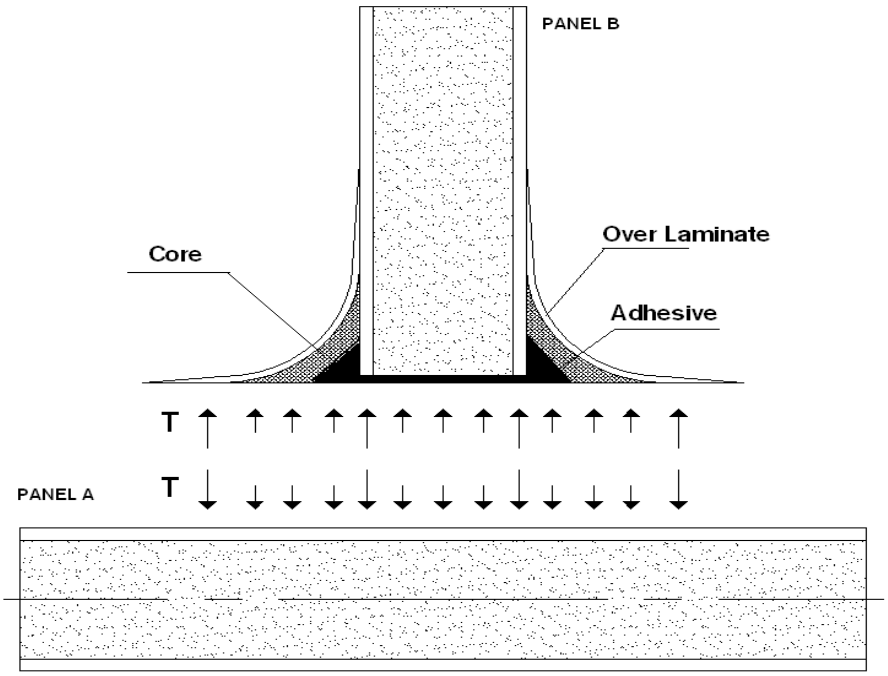


**Fig. 6.** Distribution of loads at a joint.

## 2.4. Failure of T-joints

Sandwich beams can fail from a number of different failure mechanisms, which are described by among others Zenkert [1]. Here, the most critical failure mechanisms for T-joints loaded in compression are listed based on results from previous studies; 3-point panel bending test by Steeves, Fleck [5] and T-joint compression tests by Shenoi and Violette [7]. Schematic sketches are shown in Fig. 7.

- Indentation, which is the result of a concentrated transverse load on the sandwich panel. When the yield stress is reached in the core material, it no longer supports the face which will be locally indented.

- Core shear failure from transverse shear stresses.

- Face wrinkling: local buckling of the face sheet that occurs due to compressive in-plane loading.

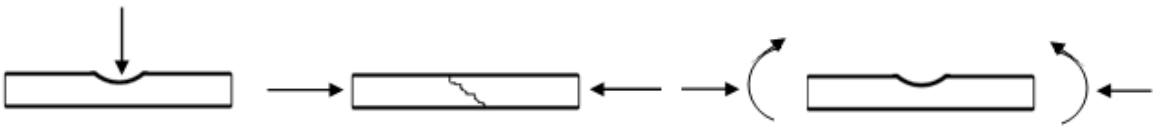

**Fig. 7.** Failure mechanisms, from left to right:
indentation, core shear failure, and face wrinkling.

## 3. Global model analysis

Vessels longer than 50 m are obliged to conduct a global strength analysis, besides the conventional strength calculations according to DNV's HSLC classification notes [10]. However, in this thesis a global strength analysis has been performed on a 23 m vessel in order to achieve realistic boundary conditions for the local strength analysis.

A global model was created in Rhinoceros according to blueprints of CarboCat [9], provided by Kockums AB. Afterwards, the geometry was exported to ANSYS, where the rest of the analysis was conducted. Shell elements were used in the FE calculations and convergence of displacement of the interested joint area was achieved with an element size of 150 mm. The material properties were provided from Kockums AB; see Table 1 and Table 2. In Fig. 8, the coordinate notations for the laminate material properties are shown. In the global model the Divinycell H80 was used as core material.

**Table 1.** Laminate material properties.

| | **Ex, Ey [GPa]** | **Ez [GPa]** | **Gxy [GPa]** | **Gyz, Gxz [GPa]** | **υxy** | **υyz, υxz** | **Sx, Sy tension [MPa]** | **Sx, Sy compr. [MPa]** |
|---|---|---|---|---|---|---|---|---|
| **Carbon fibre / vinylester** | 43 | 6 | 16.325 | 21.203 | 0.317 | 0.014 | 500 | 300 |

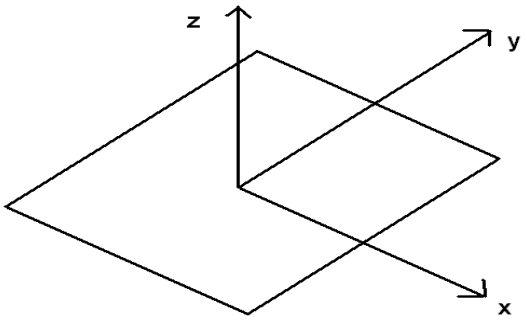


**Fig. 8.** Coordinate notation for laminate material properties.

**Table 2.** Core and adhesive material properties.

| | **E [GPa]** | **G [GPa]** | **υ** | **S tension [MPa]** | **S compr. [MPa]** | **S shear [MPa]** |
|---|---|---|---|---|---|---|
| **Divinycell H80 PVC foam core** | 0.065 | 0.023 | 0.25 | 2.5 | 1.4 | 1.15 |
| **H100 core** | 0.095 | 0.030 | 0.25 | 3.5 | 2.0 | 1.6 |
| **H130 core** | 0.130 | 0.040 | 0.25 | 4.8 | 3.0 | 2.2 |
| **H200 core** | 0.235 | 0.070 | 0.25 | 7.1 | 5.4 | 3.5 |
| **H250 core** | 0.300 | 0.087 | 0.25 | 9.2 | 7.2 | 4.5 |
| **Polyester adhesive** | 1.2 | 0.17 | 0.47 | - | - | - |

## 3.1. Load cases

According to the DNV global strength analysis classification notes [10] there are several load cases that need to be analysed. These are the conditions derived from the possible worst case scenarios which can occur in the vessel during its service life. Some of the load cases are the combination of each individual load case. Selection of which load cases need to be analysed is a matter of possible problems that can occur at the area of interest. In this thesis, cross structure of the catamaran demi-hulls are the area of main interest, and the reason for selecting this area is its being the main load carrier between two demi-hulls via frames and decks. For this reason, the load cases shown below were chosen. The first case is still-water condition. Departure lightweight of 66 tonnes was applied according to load distribution diagram. In order to achieve the desired weight distribution, the densities of the materials of the decks and hull sides were varied. This condition is the basis of load cases 3 and 4. Boundary conditions were applied as clamped node on the centreline of the catamaran at the most aft part of the weather deck, fixed in the upwards direction at the centreline of the port demi-hull at the most aft part of the weather deck and fixed in the upwards and longitudinal directions at the most fore part of the weather deck at the centreline, see Fig. 9. The reason for using these boundary conditions is to prevent rigid body motions [10]. The exception of the boundary conditions mentioned Fig. 9 is in the load case 5.To be able to implement a torsion moment, the fixed point at the demi-hull was set free.

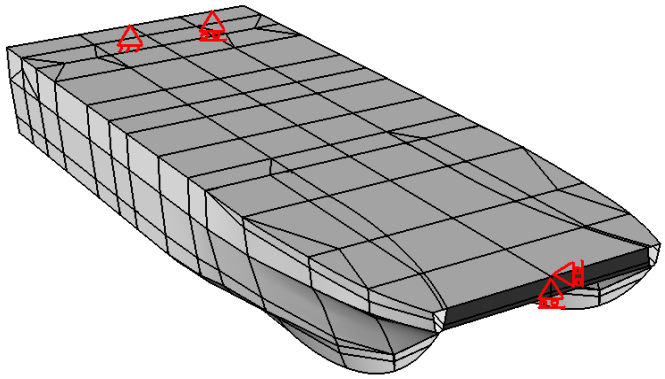

**Fig. 9.** Presentation of locations where the boundary conditions were applied on the model.

Five load cases were studied and they are described in more detail in the following sections:

1. Still-water case
2. Longitudinal sagging case
3. Transverse split moment inwards + still-water case
4. Transverse split moment outwards + still-water case
5. Torsion moment + longitudinal sagging moment case

### 3.1.1. Load case 1: still-water condition

In this condition, the still-water condition was studied. Buoyancy forces were applied as nodal forces (arrows) up to the design waterline and through LWL in length; see Fig. 10.

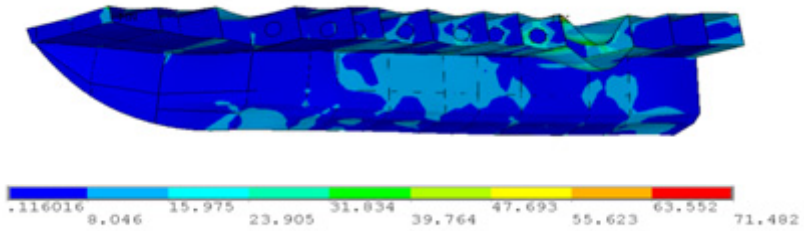


**Fig. 10.** Presentation of von Mises effective stress [MPa] for a still-water condition.

### 3.1.2. Load case 2: longitudinal sagging moment

The required sagging moment value is 2600 kNm according to DNV's HSLC rules [3]. In order to achieve this condition, the required buoyancy force was applied to fore and aft of the ship by applying nodal forces (arrows) to the fore and aft locations and to a limited extent the coupling of these forces created the required moment; see Fig. 11.

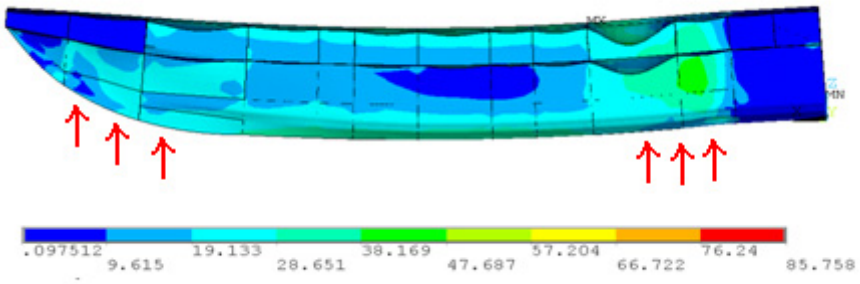


**Fig. 11.** Presentation of von Mises effective stress [MPa] for a sagging condition.

### 3.1.3. Load case 3: transverse split moment inwards + still-water

The required transverse split moment value is 764 kNm. Nodal forces (arrows) were applied to hull sides and bottom according to DNV strength analysis guideline [10]; see Fig. 12.

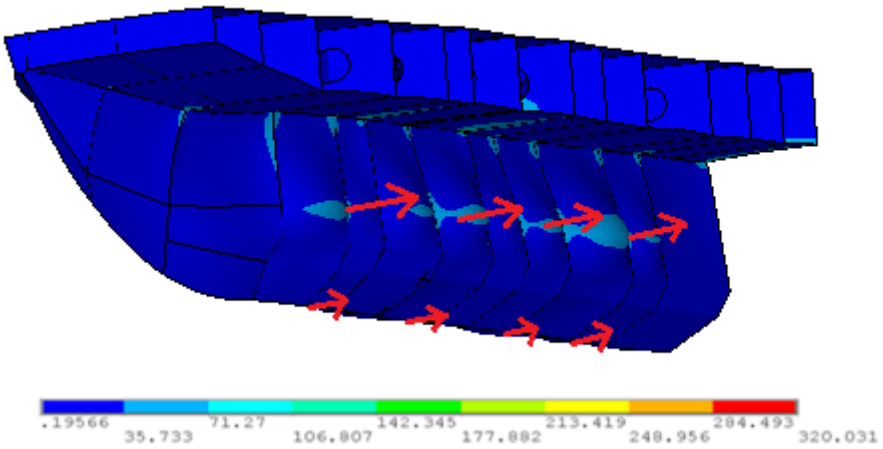


**Fig. 12.** Presentation of von Mises effective stress [MPa] for an inwards split moment and a still-water combined condition.

### 3.1.4. Load case 4: transverse split moment outwards + still-water

The required transverse split moment value is 764 kNm and it was applied from an outwards direction of the hull. Nodal forces (arrows) were applied to the hull sides and bottom according to DNV strength analysis guidelines [10]; see Fig. 13.

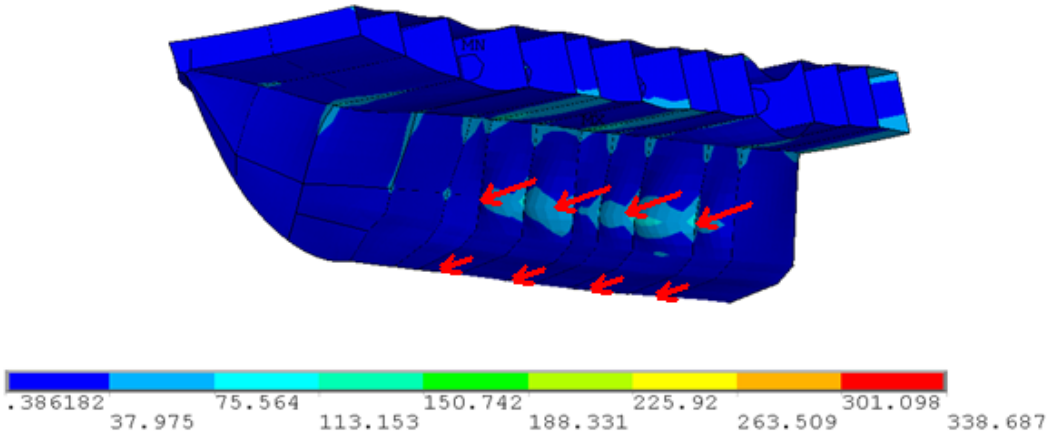


**Fig. 13.** Presentation of von Mises effective stress [MPa] for an outwards split moment and a still-water combined condition.

### 3.1.5. Load case 5: torsion moment and longitudinal sagging moment

In this condition, a torsion moment of 1242 kNm was applied in combination with a longitudinal sagging moment of 2600 kNm, by applying forces on the deck and bottom, as required by DNV strength analysis guidelines [10]; see Fig. 14.

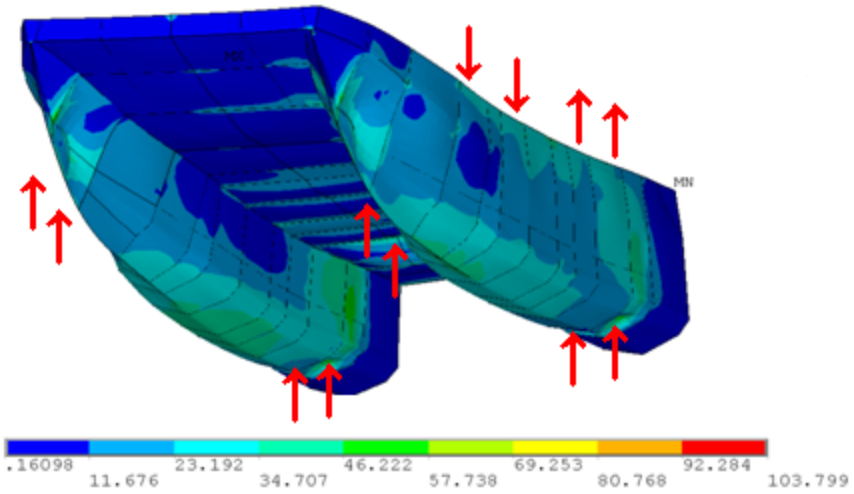


**Fig. 14.** Presentation of von Mises effective stress [MPa] for a torsion and sagging combined condition.

### 3.1.6 Identification of the critical joint and load case

In each analysis, except for the still-water condition, the critical joint of the wet deck-hull connection was evaluated. Unlike in the main deck there is a lack of continuity in the deck structure at this location, which makes it more susceptible to load effects. The results can be seen in Table 3.

**Table 3.** Highest stress values of critical joints in each condition.

| Condition | Location | von Mises effective stress |
|---|---|---|
| Longitudinal Sagging Moment | Frame 3 | 27 MPa |
| Transverse Split Moment Inwards + Still-water | Frame 6 | 114 MPa |
| Transverse Split Moment Outwards+ Still-water | Frame 6 | 148 MPa |
| Torsion Moment+Longitudinal Sagging Moment | Frame 11-Port | 29 MPa |

In Table 5, the worst cases for the joint are the *transverse split moment outwards + still-water* and *transverse split moment inwards + still-water conditions*. The former primarily leads to tensile loading of the core material in the wet deck-hull side joint, while the latter primarily leads to compressive loading of the same location. As was mentioned in Chapter 2, core materials are more susceptible to compressive failure than tensile failure. For this reason, the *transverse split moment inwards + a still-water condition* is considered to be the most critical of these load cases. This load case was selected for further evaluation via submodelling of the highest stressed joint location at frame 6.

# 4. Local model analysis

As shown in the evaluation of the global model tests in Chapter 4.1.6, below, the most critical load conditions for the T-joint in the wet deck-hull connection are the transverse bending conditions. Local FE-models were created for the critical T-joint in the wet deck-hull connection at Frame 6 where the maximum stress was found. In Fig. 15, the position of the joint on the hull is shown. The cut-out view shows the bulkhead hidden by the hull and indicates the exact location of the critical area with bold lines.

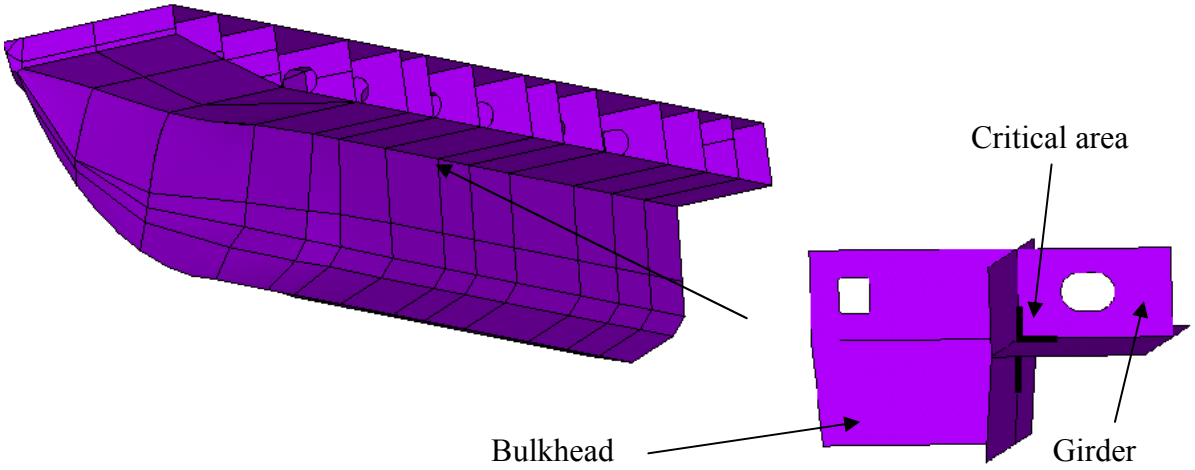


**Fig. 15.** Location and cut-out view of critical T-joint.

A 2D-model was created and used for simplified analyses of the joint. The low complexity of the model gave the possibilities to use a fine mesh and to investigate the influence of altering geometrical parameters. Additionally, a 3D-model was created as a more representative model of the actual joint, including the bulkhead and the girder which are connected at right angles to the plane of the joint and could not be modelled in 2D. With respect to the failure mechanisms described in Chapter 2.4 several result data were chosen for investigation:

- Core material compressive stress, normal or von Mises effective stress, whichever was the highest.
- Core material shear stress.
- Laminate compressive stress in the fibre direction.

## 4.1. 2D model of the T-joint

Upon closer investigation of the global model transverse bending load cases, it was seen that the main loading of the particular joint is in the plane of the joint. Relative displacements in the depth direction of the joint are small. It was therefore concluded that a 2D model could give a good representation of the joint response. The basic geometry and materials used in the model were taken from a typical T-joint configuration by Kockums. Linear, orthotropic material models were used for the laminates and linear, isotropic models for the core materials and structural adhesive. Dimensions are shown in Fig. 16 and listed in Table 4, while material properties are listed in Table 1 and 2. Divinycell H80 core material was used in the panels and H250 core material for the fillet cores. Note that the joint in Fig. 16 is rotated 90 degrees counterclockwise from the joint orientation in Fig. 15. The horizontal panel denoted as Panel A therefore represents the hull side panel while the vertical panel represents the wet deck panel.

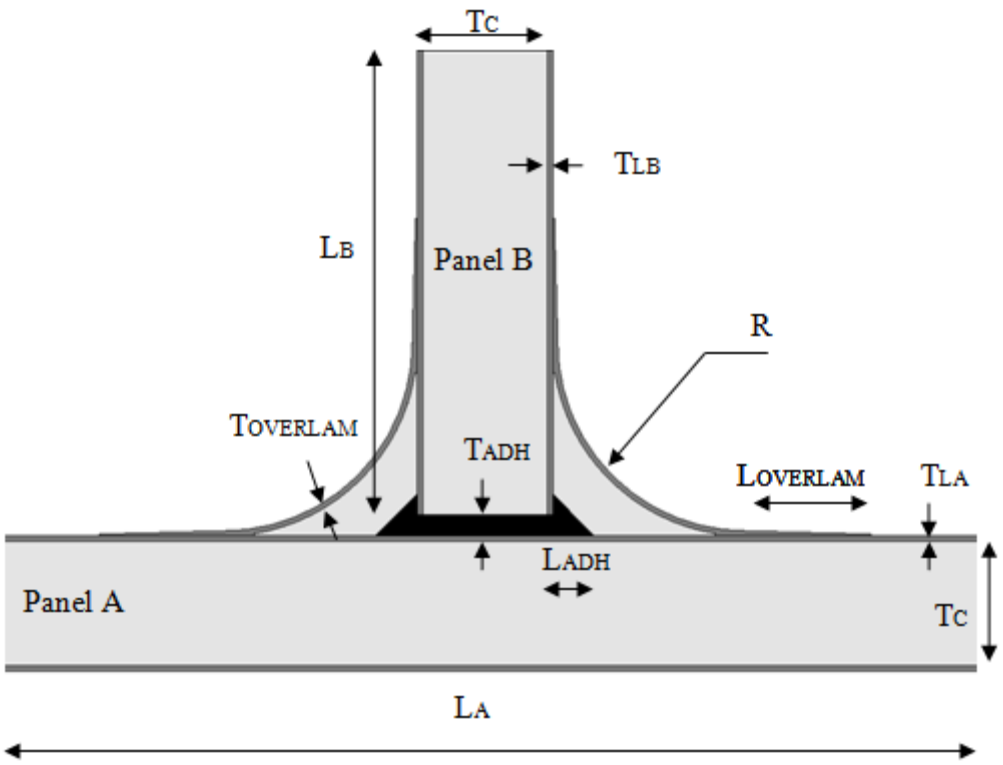


**Fig. 16.** T-joint geometry.

**Table 4.** T-joint dimensions.

| Parameter | Dimension [mm] | Description |
|---|---|---|
| $L_A$ | 600 | Panel A length |
| $L_B$ | 300 | Panel B length |
| $T_{LA}$ | 1.24 | Panel A face laminate thickness |
| $T_{LB}$ | 1.22 | Panel B face laminate thickness |
| $T_C$ | 30 | Core thickness |
| $T_{ADH}$ | 7 | Adhesive thickness |
| $L_{OVERLAM}$ | 30 | Overlaminate overlap length |
| $L_{ADH}$ | 10 | Adhesive overlap length |
| R | 60 | Overlaminate radius |

The mesh was created from the eight-node quadratic element plane 82 which was used successfully in [6]. After a convergence study comparing core material maximum compressive stress, an element side length of 1.24 mm (equal to the laminate thickness) was considered sufficient for the model. The mesh consists of about 21000 elements and is shown with shortened panels in Fig. 17. At each panel end very stiff beam, elements were created to connect a master node outside of the geometry to the slave nodes on the edge. This master-slave boundary modelling allows a simple application of displacements and loads. In order to achieve correct alignment of material properties, additional local coordinate systems were created to control the element coordinate systems.

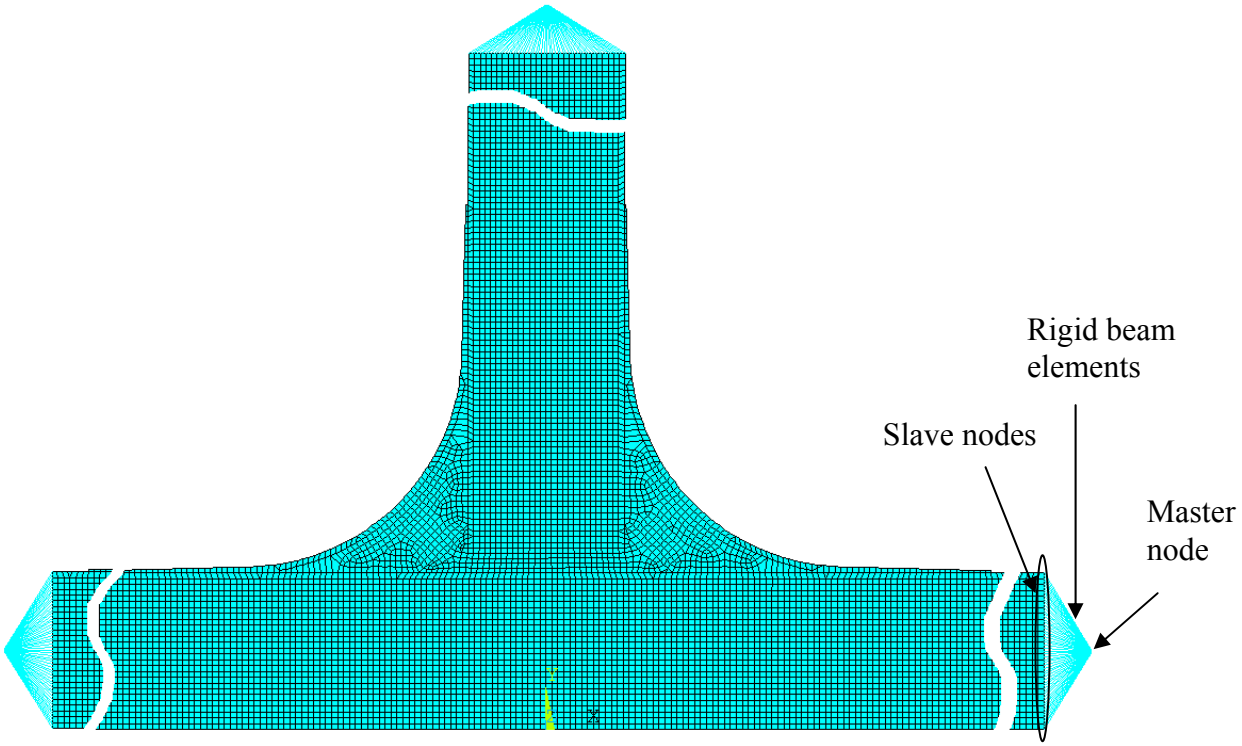


**Fig. 17.** T-joint mesh.

Two types of calculations were run with the 2D-model: submodelling of the critical load case and simplified load tests with the purpose of determining the load-distributing effect of the joint components as well as the influence of geometrical dimensions on the load distribution.

### 4.1.1. Submodelling

The method employed for submodelling was to extract displacements from nodes around the joint in the global model and apply these to the master nodes in the local model. Figure 18 shows the global model mesh surrounding the critical joint. The three nodes where displacements were read are displayed. Relative to the centre of the joint these are located in the same positions as the master nodes in the local model.

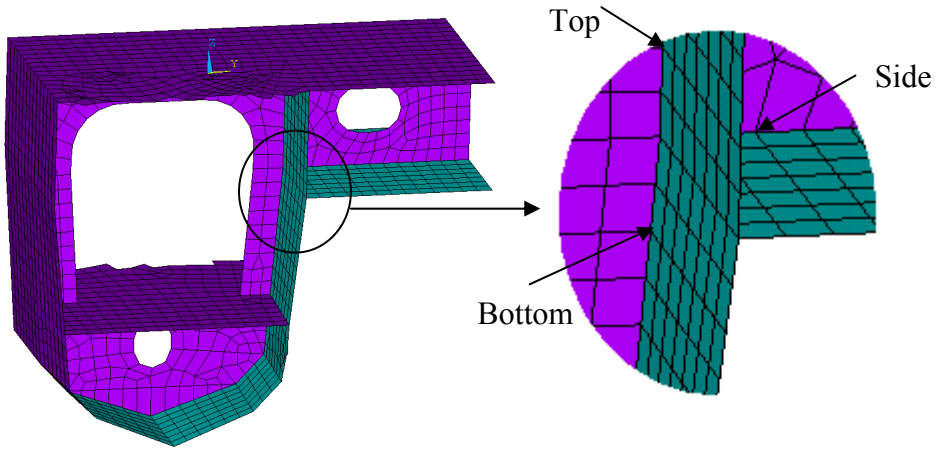


**Fig. 18.** Nodes used for extraction of displacements.

The displacements read from the global model were transformed into the coordinate system of the local model and normalised with respect to the top master node before they were applied to the respective master nodes. The top master node would then become a reference node in the calculations. A schematic view of the displacements for the two load conditions is shown in Fig. 19.

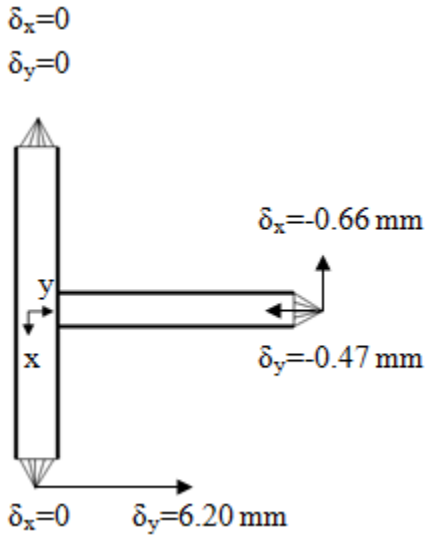


**Fig. 19.** Application of displacements, inwards transverse, split moment conditions.

It was suspected that the joint deformation in this submodel would not be realistic without including the bulkhead and the girder which are adjacent to the joint. Therefore, a second model was made where these were included. The bulkhead and girder are sandwich panels which also have a depth dimension. This could not be modelled in 2D, but the 2D model does, instead, represent a cut in the plane of one of the laminates in the bulkhead and girder. Displacements from the global model were applied both to the master nodes and to the edges of the bulkhead and girder as seen in Fig. 20.

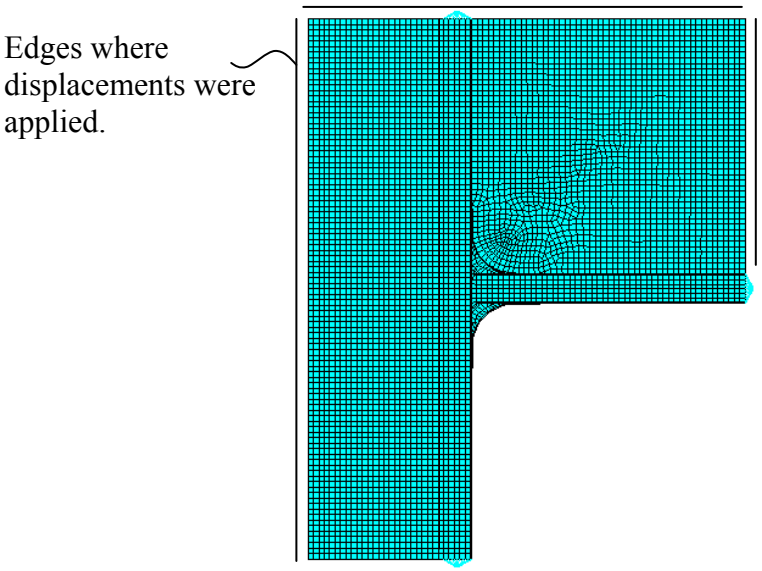


**Fig. 20.** 2D FE model of the T-joint including bulkhead and girder.

For both models, compressive stress in the y-direction, the von Mises effective stress and shear stress were investigated for the core material of Panel A. Laminate stress in the fibre direction was also investigated. Stress results are listed in Table 5 together with material utilization which is defined in Eq. (10). The term *material utilization* refers to how high the stresses are in relation to the allowed stresses. By comparing material utilization it can easily be shown which stress is the most critical despite there being different strength values for the different stresses.

$$Material \quad utilization = \frac{\sigma \cdot R}{S} \tag{10}$$

where:
$\sigma$ = actual stress value
$R$ = DNV safety factor, $R$ = 3.3 [3]
$S$ = material strength, listed in Table 1 and Table 2

**Table 5.** Resulting stresses from 2D submodelling.

| | **Without bulkhead** | | **With bulkhead** | |
|---|---|---|---|---|
| | **Stress [MPa]** | **Material utilisation** | **Stress [MPa]** | **Material utilization** |
| Core $\sigma_{max\ compression}$ | 0.30 | 71% | 5.47 | 1290% |
| Core $\sigma_{max\ von\ Mises}$ | 0.50 | 118% | 5.08 | 1200% |
| Core $\lvert\tau_{max}\rvert$ | 0.29 | 83% | 0.97 | 278% |
| Laminates (fibre dir.) $\sigma_{max\ tension}$ | 39 | 26% | 168 | 111% |
| Laminates (fibre dir.) $\sigma_{max\ compression}$ | 45 | 50% | 233 | 256% |

Figures 21 and 22 show the deformed shape of the models and plots of compressive stress in the y-direction of the core material in Panel A. The deformations are magnified. As can be seen, much higher stresses were achieved for the model that includes the bulkhead and girder. In that model the core material of Panel A could be seen to be compressed between the bulkhead and the wet deck, while in the simpler model the joint area was seen to deflect in the negative y-direction without the bulkhead restricting the motion.

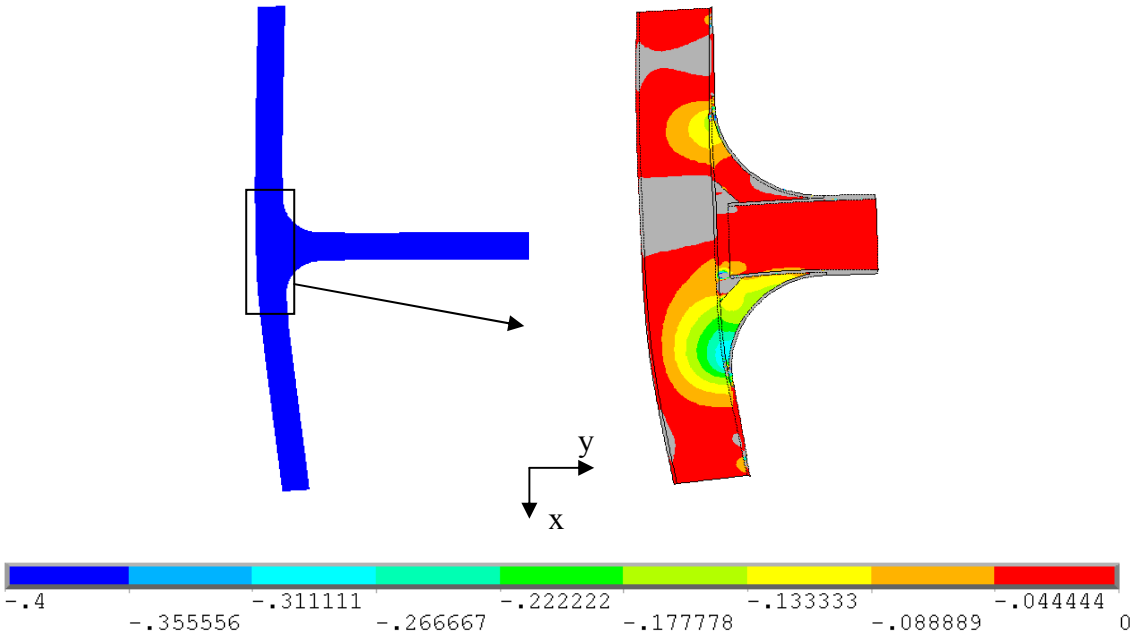


**Fig. 21.** 2D submodel deformation shape and plot of y-direction compressive stress [MPa].

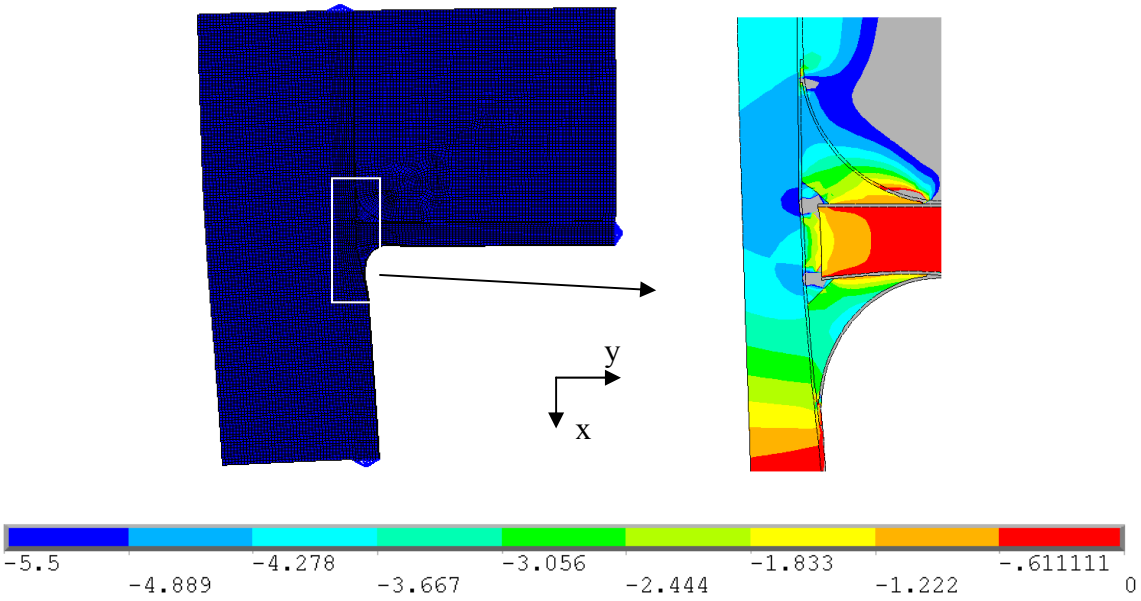


**Fig. 22.** 2D submodel with bulkhead deformation shape and plot of y-direction compressive stress [MPa].

### 4.1.2. Stress distribution tests

In the stress distribution tests, joint geometry and materials were altered for different boundary and load conditions. Two types of boundary conditions were used: fixed bottom by fixing all nodes at the bottom boundary and simply being supported by fixing translations at the left and right master nodes. Compressive and bending loads were achieved by applying a force to the top master node, either vertically or horizontally. The combinations of boundary and load conditions are displayed in Table 6.

**Table 6.** Combinations of boundary and load conditions.

| | Fixed | Simply supported |
|---|---|---|
| **Compression** | 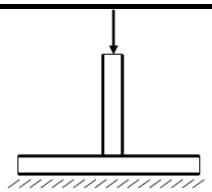 | 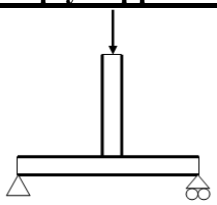 |
| **Bending of Panel B** | 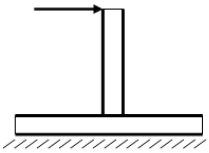 | 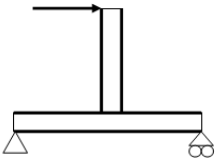 |

The initial tests were made by step by step adding the components of a joint to show the influence of each component on the stress distribution in the core material. A schematic overview of the tests is shown in Fig. 23. Dimensions and material properties were used according to Table 4, Table 1 and Table 2 using an H80 core in the panels and an H250 core for the fillet cores.

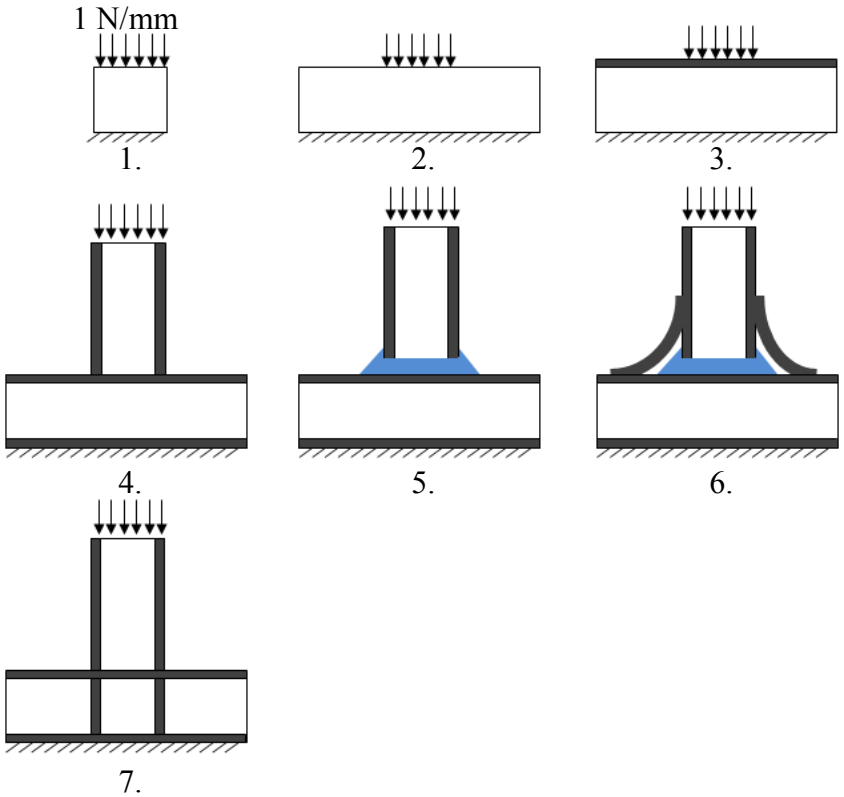


**Fig. 23.** Schematics of stress distribution tests.

(1) For the reference case, an assumption was made that the entire joint is rigid except for the core material situated directly below the vertical Panel B (a rectangular piece w × h = 32.48 mm × 30 mm). A compressive load at the top of the joint would then be taken up only by the considered piece of core material. It is easily realised that a load of 1 N/mm would result in a vertical compressive stress equal to 1 MPa through the entire piece of core material, which was confirmed by the FE-results.

(2) The width of the core material was extended, while a distributed load of 1 N/mm was still applied along 32.48 mm of the top boundary.
(3) Same as Test 2 with laminates added.
(4) Panel B is introduced to show the stress concentrations below the laminate intersections. A point load, which is equivalent to the distributed load, is applied to the top master node for this test and the following ones (F = 1 N/mm × 32.48 mm = 32.48 N).
(5) Introducing the structural adhesive.
(6) Introducing overlaminates.
(7) Panel B laminates are extended to show an example of a joint with laminate continuity.

Following the initial compression tests, Tests 4-7 were performed with an altered boundary and load conditions according to Table 6. The force applied for a bending load was set so that the normal force onto the core material from the laminate on the compressed side would be equal to the force during compressive loads. From a moment balance it can be seen that the applied force should be $F \times T_C/L_B$.

Results in the form of maximum y-direction compressive stress, von Mises effective stress and shear stress in the core material of Panel A are listed in Tables 7 and 8. The y-direction stress plots for the compression tests with a fixed bottom boundary are shown in Fig. 24. It can be seen how a wider piece of core material and the addition of laminates help distributing stresses in Tests 1-3. The formation of stress concentrations is shown in Test 4 and it can then be seen how stresses become gradually more distributed in Tests 5-7. It is clearly shown that maximum stress values are reduced and that a larger cross sectional area of the core material carries the load when the adhesive and overlaminates are introduced to the joint. As expected, the load carried by the core in the joint with continuous laminates is negligible.

The most interesting comparison is to compare the results for Test 6 to those for Test 4. For the fixed bottom-compression condition the compressive stress can be seen to be reduced from 0.97 to 0.30 MPa. From the results for the simply supported-compression condition it can be seen how the overlaminate joint geometry in Test 6 reduces stresses less efficiently in comparison to the Test 4 condition, while for both bending conditions it can be seen to give a higher stress reduction.

**Table 7**. Compression load conditions: maximum vertical compressive stress, von Mises effective stress and shear stress in the core material of Panel A [MPa].

| | **Boundary conditions** | | | | | |
|---|---|---|---|---|---|---|
| **Test #** | **Fixed** | | | **Simply supported** | | |
| | $\sigma_{max\ comp.}$ | $\sigma_{max\ VM}$ | $\lvert\tau_{max}\rvert$ | $\sigma_{max\ comp.}$ | $\sigma_{max\ VM}$ | $\lvert\tau_{max}\rvert$ |
| 1 | 1.00 | - | - | - | - | - |
| 2 | 1.11 | - | - | - | - | - |
| 3 | 1.00 | - | - | - | - | - |
| 4 | 0.97 | 0.93 | 0.20 | 1.08 | 1.17 | 0.55 |
| 5 | 0.62 | 0.57 | 0.14 | 0.83 | 1.02 | 0.55 |
| 6 | 0.30 | 0.28 | 0.04 | 0.57 | 0.79 | 0.45 |
| 7 | 0.05 | 0.06 | 0.03 | 0.34 | 0.91 | 0.53 |

**Table 8**. Bending load conditions: maximum vertical compressive stress, von Mises effective stress and shear stress in the core material of Panel A [MPa].

| | Boundary conditions | | | | | |
|---|---|---|---|---|---|---|
| **Test #** | **Fixed** | | | **Simply supported** | | |
| | $\sigma_{max\ comp.}$ | $\sigma_{max\ VM}$ | $\lvert\tau_{max}\rvert$ | $\sigma_{max\ comp.}$ | $\sigma_{max\ VM}$ | $\lvert\tau_{max}\rvert$ |
| 4 | 1.08 | 1.05 | 0.23 | 1.06 | 1.13 | 0.50 |
| 5 | 0.60 | 0.57 | 0.15 | 0.59 | 0.66 | 0.37 |
| 6 | 0.15 | 0.14 | 0.04 | 0.11 | 0.27 | 0.16 |
| 7 | 0.06 | 0.07 | 0.03 | 0.20 | 0.80 | 0.46 |

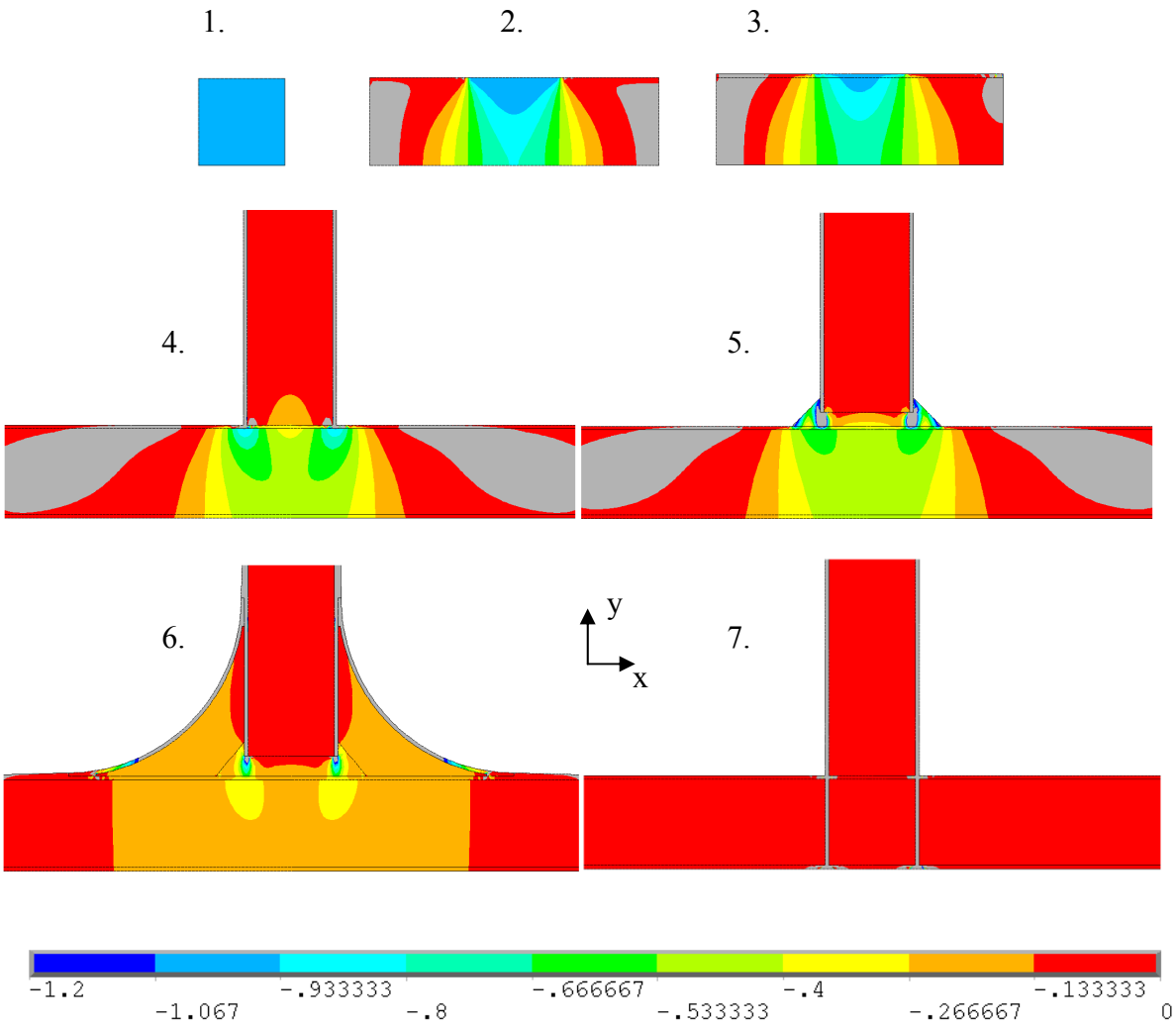


**Fig. 24.** Plot of y-direction compressive stress [MPa] for Tests 1-7 with a fixed bottom boundary.

### 4.1.3. Parametric studies

Parametric studies were conducted on the local 2D-model with the aim of assessing the influence of design parameters on a joint's load-carrying capability. The study was done in accordance with Test 6 in Fig. 23 – a general compression load test with a fixed bottom boundary. The initial reference dimensions were taken from Table 4 and materials from

Table 1 using H80 panel core material and H250 fillet core material. Tests were then conducted altering one parameter at the time while investigating the resulting compressive stresses in the core material of Panel A. The parameters which were found to be most influential are presented below. The plotted compressive stresses were normalised to the stress achieved with the reference parameters (0.30 MPa that was achieved in test 6).

The overlaminate radius is one of the most obvious joint design parameters. A larger radius distributes the load over a larger cross section of the core material in Panel A. It should be noted that for radii smaller than 40 mm, a structural adhesive was used as filler material under the overlaminate instead of fillet core material. This is common practice at Kockums. It can be seen in Fig. 25 that well over a 10% stress reduction can be achieved by going from a 60 mm to 80 mm radius.

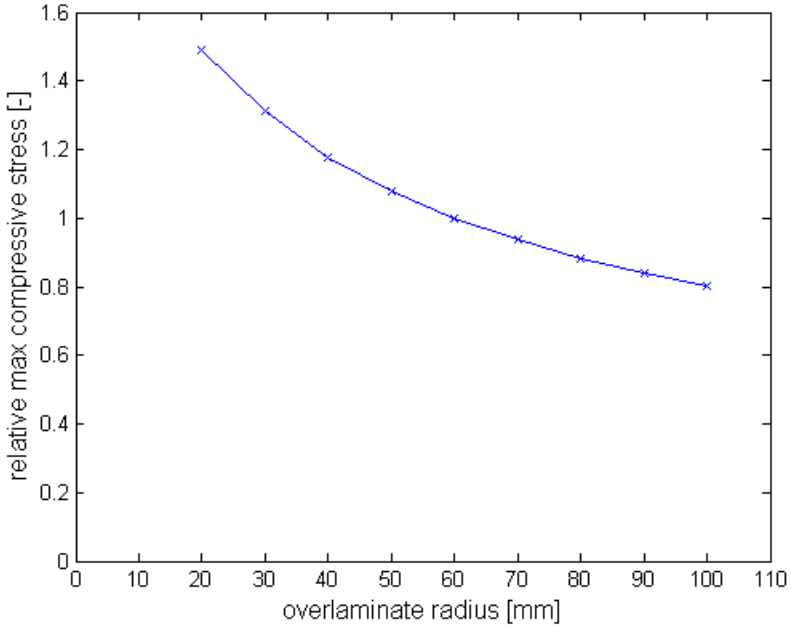


**Fig. 25.** Relative maximum compressive stress in the core material of Panel A as a function of overlaminate radius.

The structural adhesive layer between the vertical and horizontal panel laminates also has a well-known functionality. Even when the joint has a large overlaminate radius, the major part of the load is still transferred via the Panel B laminates through the structural adhesive for vertical compressive loads. Since the adhesive has a much lower stiffness than the laminates, it deforms and distributes the load over a larger cross section. As can be seen in Fig. 26, a thicker adhesive layer allows for a better load distribution. Doubling the thickness from the reference thickness from 7 mm to 14 mm would yield a 7-8% stress reduction.

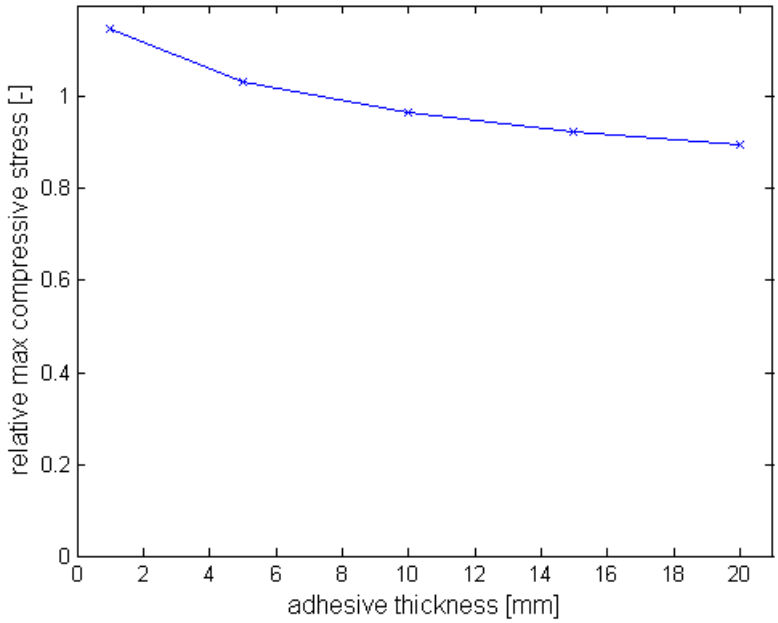


**Fig. 26.** Relative maximum compressive stress in the core material of Panel A as a function of adhesive thickness.

Another important design parameter is the core material itself in Panel A. The Divinycell PVC foam core comes in several density steps where both stiffness and strength increases with density. In tests, it could be seen that higher stiffness gives higher core material stresses. Therefore, to account for change in both strength and stiffness the change in material utilisation was evaluated, here defined as stress/strength. The H80, H100, H130, H200 and H250 core materials with properties listed in Table 2 were investigated and it can be seen in Fig. 27 that the material utilisation is lowered by almost 70% by going from H80 to H250.

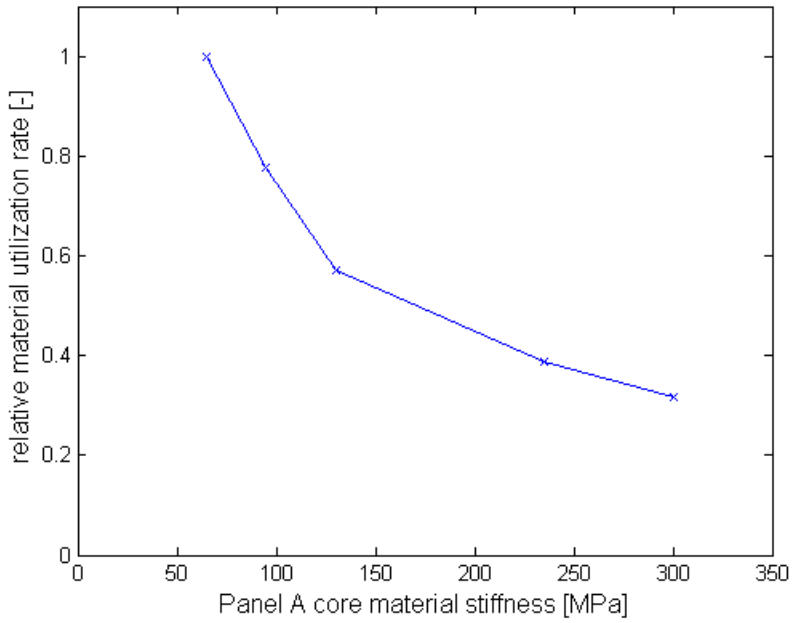


**Fig. 27.** Relative material utilization as a function of Panel A core material stiffness.

## 4.2. 3D model of the T-joint

In order to observe the effect of the joint geometry and the selection of core material, the actual joint geometry was modelled in 3D. The reason for conducting a 3D analysis as well as a 2D analysis was to be able to more accurately observe the effect on the joint stress distribution from the bulkhead and girder at the joint location. Besides, an additional purpose was to observe the differences between 2D modelling and 3D modelling. It was investigated under what kind of circumstances the use of 2D modelling is sufficient and when the more complex 3D modelling is required. The approach of 3D modelling involves many obstacles in itself. These obstacles create a lot of difficulties and require attention. First of all, the joint geometry is not as simple as in the 2D model. Another important point to be careful about is the mesh quality at the area of interest in the model. For example, the stress values read from solid wedges elements are unreliable to read. This is due to insufficient characteristics of the solid elements at the wedges.

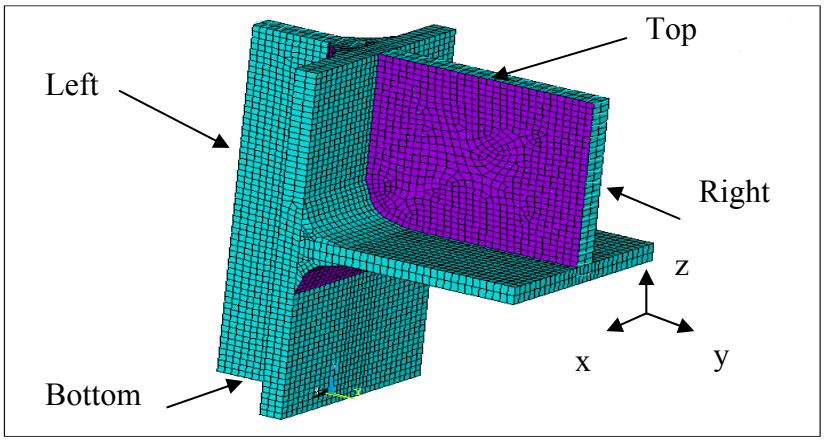


**Fig. 28.** 3D joint mesh

In the 3D analysis a solid-shell modelling technique was employed. The core and adhesive materials were modelled as solid 95 elements in ANSYS. The laminates were modelled with the shell 281 element. The dimensions and materials were set to the same as were used for the 2D submodelling, see Table 4, Table 1 and Table 2. The mesh is separated into two groups, one that consists of the elements closest to the area of interest and one that consists of the remaining elements. This gives the possibility to achieve accurate results while keeping the computational time at reasonable levels. A convergence study was conducted that concluded an element side length of 4 mm in the area of interest and 10 mm to be sufficient for accurate results. The study can be seen in Appendix A. There exist a few solid wedges in the mesh, but not in the area of interest. The boundary conditions were extracted from the global model. In order to simplify the calculation procedure, boundary conditions were not employed on all the edges of the joint. Boundary conditions were extracted for the bottom, top, right and left edges of the joint and were applied to master nodes on very stiff shell elements on these edges, see Fig. 28. These locations were chosen because of their importance regarding representing the behaviour of the joint. As was mentioned in Chapter 4.1 the inwards transverse bending load case mainly implies deformation in the plane of the joint (the y-z plane in Fig. 28). Since boundary conditions are applied to the edges of panels that are stiff in the plane of the joint, the actual deformation should be represented fairly well.

Initially, the geometry (radius of the fillet and overlaminate) and the core material at Panel A, which is the hull side, were modified according to three different radii and three different types of core material. The thickness of the overlaminate was not altered; Theotokoglou and

Moan [13] concluded that it does not have significant importance at an ultimate load-carrying capacity. According to this study, it can be stated that radius and type of core material have as enormous an importance regarding distribution of the load as for the stress values. First of all, it was observed that stresses at the laminate and shear stresses at the core are not the decisive stresses in the joint design. In all of the cases, these stresses are within the limit of allowable stress values. However, compressive stresses, as it is supposed, are the critical decisive stresses.

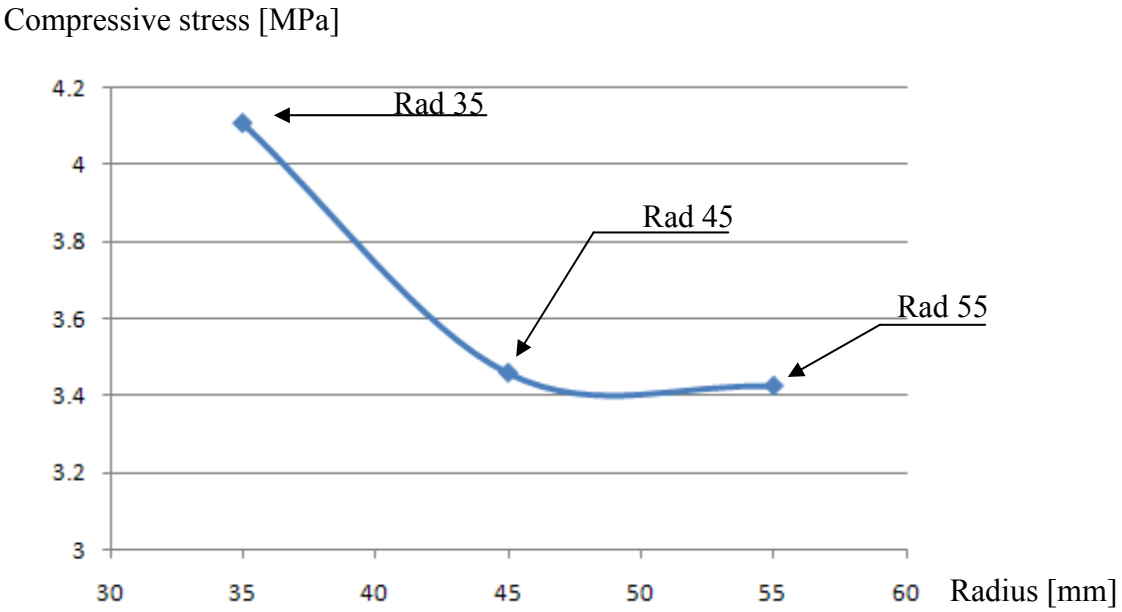


**Fig. 29.** Compressive stress versus radius.

As seen in Fig. 29, the large radius decreased the peak stress value significantly. Another parametric study has been conducted to see the effect of the core material type at the joint on Panel A with a constant radius of 55 mm.

**Table 9.** Compressive stress for various core materials.

| Core types | $\sigma_{max\ comp.}$ [MPa] | Allowable compressive stresses [MPa] with safety factor | Material Utilization |
|---|---|---|---|
| **H 80** | -3.423 | -0.425 | 805% |
| **H130** | -4.269 | -0.91 | 469% |
| **H250** | -6.579 | -2.18 | 301% |

As can be seen in Table 9 the core material also plays an important role in joint design as well as the radius. However, the stress values are still higher than allowable compressive limits. The existence of the bulkhead and wet-deck intersection creates high stress concentrations, see Fig. 30.

Compressive stress plots can be seen in Appendix B. However, these are the results of coarser meshes and the aim is to present the trend of stress. The result of a finer mesh can be seen in Table 17.

Figure 30 shows the resulting stress distribution in the core material of the joint when the design parameters that were found to perform best in the parametric study are used. That is,

H250 core material in the joint and a 60 mm overlaminate radius. It can be seen that the maximum compressive stress occurs where the aftmost laminate of the bulkhead meets the hull side. The resulting maximum stresses (read at the location shown in Fig. 30) and material utilization, as defined in Eq. (10) are listed in Table 10.

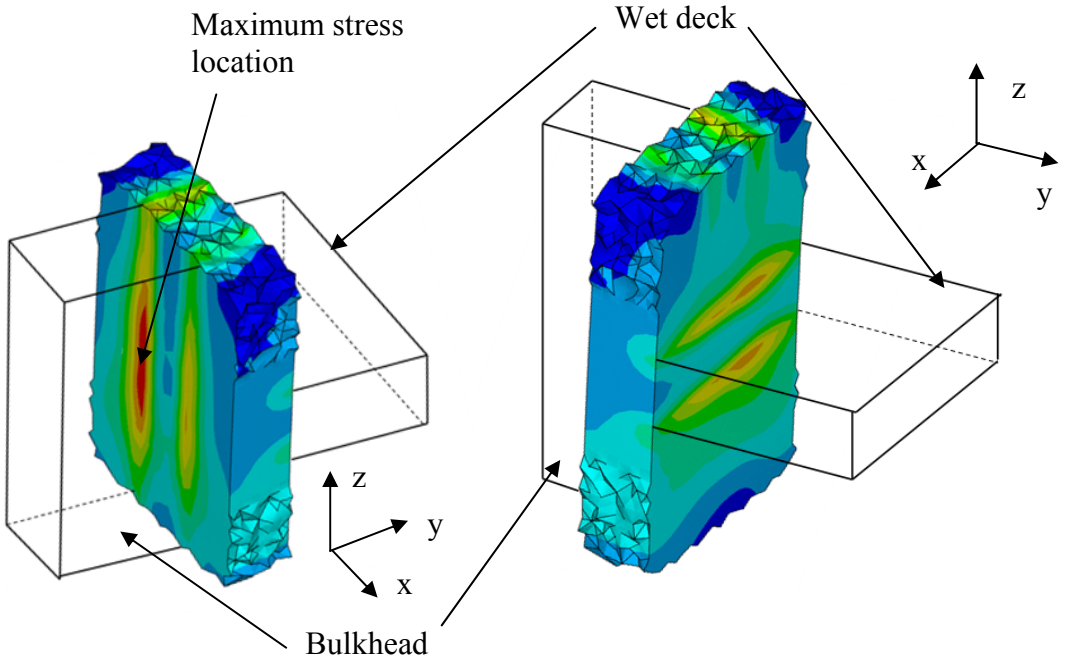


**Fig. 30.** 3D model – plots of stress intensity for y-direction compressive stress in the core.

**Table 10.** Resulting stresses from 3D submodelling with core H250 and radius 60 mm.

| | **Stress [MPa]** | **Material utilization** |
|---|---|---|
| Core $\sigma_{max\ compression}$ | 9.69 | 440% |
| Core $\sigma_{max\ von\ Mises}$ | 6.92 | 317% |
| Core $\lvert\tau_{max}\rvert$ | 1.14 | 84% |

## 4.3 Comparison between 2D and 3D model results

The results from the 2D model with bulkhead and girder and the 3D model are listed for comparison in Table 11 and plotted in Fig. 31. The y-direction compressive stress is used for the comparison because it is the stress that entails the highest material utilisation. It should be noted that the z-direction of the 2D model has a different orientation than in the figure. In the comparison, the H80 core material was used and an overlaminate radius of 60 mm.

**Table 11.** Comparison of y-direction compressive stress between the 2D and 3D models.

| | **$\sigma_{max\ comp.}$ [MPa]** | **Material utilization** |
|---|---|---|
| **2D model** | 5.47 | 1290% |
| **3D model** | 3.75 | 884% |

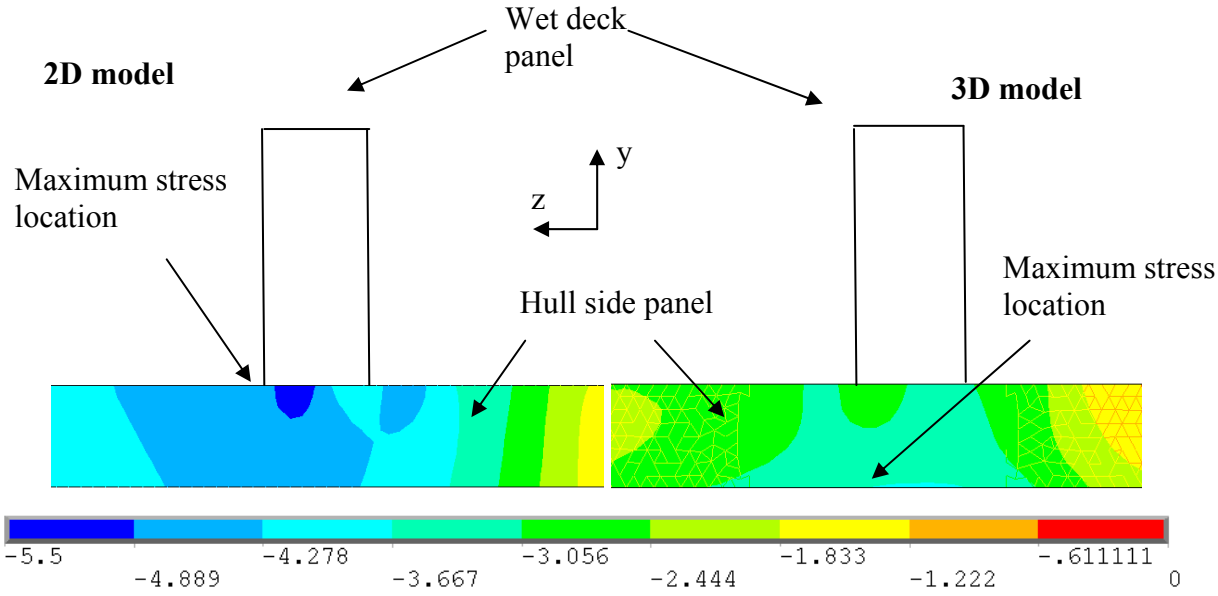


**Fig. 31.** Comparison plot of y-direction compressive stress between 2D and 3D models [MPa].

It can be seen how the stresses are higher in the 2D model and that the maximum stress locations differ. In the 2D model the maximum stress location is found at the stress concentration where the load from the upper laminate of the wet deck is transferred through the core. In the 3D model, however, the maximum stress location is found at the stress concentration where the load from the aftmost laminate of the bulkhead is transferred through the core (as can be seen in Fig. 30). Because the bulkhead laminate has no depth dimension in the 2D model no stress concentration arises at this location.

## 4.4. Proposal of design guidelines

As can be seen from Chapter 4.1 and 4.2 the core material and joint geometry prove to contribute a lot to the distribution of stresses. Starting from a given reference geometry, such as the one that was studied in Chapter 4.1.3 as well as using fixed bottom boundary conditions for Panel A, one could predict that the core material stresses from a compressive load onto Panel B would be around 30% of the applied pressure in analogy with the results for Test 6. The plots in Figs 25 - 27 show within which ranges stresses the load-carrying capability could be further scaled by varying the most influential design parameters.

The bending loads and simply supported boundary conditions were not studied in as much detail as the fixed bottom-compression condition. However, as can be seen in Table 8, the overlaminate geometry is efficient in reducing core material stress from bending loads. Conditions where the panel is represented by simply supported boundary conditions are more difficult to predict, since the stresses from the overall bending of the panel have an influence. It was seen, however, that the stress-distributing effect of the joint geometry is less efficient for simply supported boundary conditions. This is possibly due to the fact that the entire joint is displaced downwards and the overlaminates are placed in an unfavourable angle.

When it comes to more complex joint geometries, such as the studied bulkhead-wet deck connection point, stress concentrations arise and it is necessary to take extra precautions. Despite large overlaminate radii and the use of denser core material at the joint location, the

trend of the results from the study in Chapter 4.2 shows that it is not possible to pass the criteria for safe structural requirements with a regular overlaminate joint design. In order to pass the requirements, laminate continuity would be necessary. Face laminate penetration through the panel would relieve the core material from normal stresses.

Another proposal for this particular joint is the allocation of large brackets between two frames in order to mimic the fixed bottom boundary conditions that were already mentioned. The boundary conditions in this study are neither completely fixed nor completely simply supported due to the complex geometry and loading, but it is believed this solution would help minimize the high-stress values in the core.

Finally, the selection of joint type for specific locations is a question of finding out high-stress locations on the hull. Generally, a regular joint geometry and core material allocation will be enough. On the other hand, high stress locations should be constructed via a high radius and denser core material. Moreover, at the stress-concentrated areas the laminate continuity or extra brackets should be provided. In that sense, production techniques and easiness should be taken into account. Suitable techniques and joint design should be selected.

# 5. Discussion

The results from this thesis showed that the core material and joint geometry generally distribute loads very well. However, high core material stresses were seen in the study of the critical joint. This joint has rather complex and extreme features. In the intersection where the bulkhead and the wet deck are joined to either side of the hull panel, a very small cross section of core material in the hull panel has to carry a high load. Even by improving the load-carrying capability via core material selection and a larger overlaminate radius, it would not be possible to achieve stress values that fall below the allowed limits. At this joint either laminate continuity is needed or larger structural members, such as brackets that distribute the loads over a larger area, are needed.

The parametric studies showed positive results for controlling the load-carrying capability of the joint with geometrical parameters and material selection. Two important aspects that were not discussed in this thesis is the influence of cost and weight on the selection of joint design. From Kockums point of view, it is more complicated to construct a joint with laminate continuity than to construct a fillet – an overlaminate joint. However, the latter joint type has a higher weight since additional geometry is necessary to distribute the loads. Some important limitations on the design parameters that were studied are that large overlaminate radii entail high manufacturing as well as material costs and that high density core materials are much more expensive than regular core materials. Ultimately, many factors have to be weighed into the design of joints.

Submodelling as a technique requires many steps to be gone through from global modelling to local modelling. When evaluating the results the effect from each step has to be considered. In this thesis a global shell model of the vessel was created. For calculation-time reasons it would not be possible to include all details in this model. For example, joint geometry was not modelled, making the structure less stiff and therefore making displacements larger than they would otherwise have been. From that aspect the displacements that were used for submodelling are conservative. The load cases applied to the global model in accordance with classification notes are also conservative in order to make up for the fact that the loads in reality are dynamic rather than static.

Three different local models were created with different level of representation of the actual joint geometry. The first 2D model would represent a regular T-joint, the second 2D model would represent a T-joint with a bulkhead studied at a cut in the plane of one of the bulkhead laminates, while the 3D model represents the full geometry of the actual joint. For all three models boundary conditions were only applied at selected boundaries. It would be more conservative to apply boundary conditions to all boundaries. The difference in geometrical representation is believed to be the reason for the differing results between the models. In the initial modelling phase it was believed that the bulkhead and girder would not have a large effect on the structural response. After the 3D model had been created it could be seen that the location of the maximum core stress is at the joint were the bulkhead meets the hull side, this joint being out of plane of the 2D models and could therefore not be represented correctly by them. Despite this, the 2D model with bulkhead and girder showed the highest stress results. It is believed that the reason is that the bulkhead and girder laminates are modelled without a depth dimension, while, in reality, they are thin relative to the core that takes up the load. While the 3D model constitutes the best geometrical representation of the joint, it has a coarser mesh than the 2D models, possibly giving lower accuracy in the results. This could also be a further explanation for the difference in stress magnitudes. However in the

convergence study that was made for the 3D model there is only a deviation of a few per cent of the observed results for different element sizes.

Another topic that needs to be considered is the safety factor. Due to the nature of unknowns of composite materials and production imperfections, safety factor demands are high despite the fact that highly specific and detailed analyses are conducted. The requirements for safety factor can be minimised with more knowledge of the material and precision in the manufacturing process.

# 6. Conclusions

This thesis concerns the design of composite sandwich joints with a focus on the load-carrying capabilities of the core materials and joint geometry using realistic load conditions on a ship. An FE submodelling technique was employed that allowed for a good representation of the global structural response as well as detailed analysis of the area of interest. Two 2D local joint models and one 3D model were analysed and compared. 2D analyses are rather simpler and require less solution time than 3D analyses. That is why a possibility of employing 2D modelling instead of 3D modelling will save of a lot of time and money. However, it was observed that 2D modelling is not feasible for representing the actual situation very well. Stress values and locations at the joint varied between two techniques. Out of plane effects should be taken into account. 3D modelling is a more accurate way of investigating these kinds of locations where complex and discontinuous geometries are allocated. The 3D model proved to be the most representative of the studied joints by incorporating more elements of the real geometry. 2D modelling was considered to be sufficient for studying simple joints in parametric studies where continuity of the structure (out of plane direction) can be observed. A slice taken out from the structure can be regarded as being sufficient for 2D representation.

The study of the critical joint showed very high stress values in the core material. The joint that was chosen for study, transfers large loads over a small area where a bulkhead meets the wet deck. This particular joint is not suited for a joint design that has laminate discontinuity without making additional structural arrangements. Laminate continuity would definitely improve the joint characteristics considerably. Another alternative could be the allocation of large brackets between the frames that secure a more effective distribution of loads through the hull side panel. The selection of either bracket or continuous laminate is a question of manufacturability, the cost of each technique and, of course, the capability of stress reduction.

The core material and joint geometry were found to have large effects and benefits in terms of load distribution. The radius of 45 mm and an H80 core material combination give adequate stress values for regular connection points. As can be seen in Fig. 24, fillet radius and core material distributes the load effectively. When it comes to joints at more highly stressed locations, the allocation of a larger radius and a denser core material at the joint improves the joint effectively. Employing H250 core material and radius of 55 mm combination instead of H80 core material combined with a radius of 35 mm improved the design 3 times in terms of decisive stress.

An assessment of which joint type should be used at a particular location needs careful stress evaluation of the hull. One desired outcome of the thesis was to make a simplification of the studied joint, and, by using simple design rules, determine the necessary joint design. From the evaluation of the joint it was concluded that joints of this complex type and at other critical positions should be considered individually and in detail. It has been found that joint type selection is not a straightforward and easy process. Conversely, it is a very important task and extra attention is needed, especially for the catamaran type of vessels.

# 7. Future work

Regular T-joints have been investigated for a long time with detailed FE analyses and tests. Studies to optimise these kinds of joints for various loading scenarios and the results of studies can be found in literature on the subject. However, joints of interest in this study were not studied as much as regular connections. The knowledge of this type of joint is relatively limited. Due to this reason, stress concentrations at these locations needed to be investigated further. Especially, the proposals mentioned in Chapter 4.4 and Chapter 6 should be investigated thoroughly. It should be noted that in the study of bracket allocation between frames, a global model and the analysis needs to consider the existence of these brackets since it will affect the overall stress distribution.

Another very important issue is the gap between stresses evaluated from theory and stresses from FE calculations. The beam theory does not take into account joint geometry. Because of this, explicit hand calculations should be considered as conservative. On the other hand, FE analyses are costly and time-consuming. In order to achieve a rapid and reliable evaluation of the joint in question, a simpler tool is needed. This tool can be developed via a comparison of numerous FE analyses and explicit hand calculations. An example of the approach for using explicit hand calculations would be to use the beam theory combined with an elastic foundation model as for example the one described in [4] for simple cases. This tool would be very appreciated and highly needed in marine industry.

# 8. References


[1] Hertzberg T. et al. (2009). LASS – Lightweight Construction Applications at Sea. SP Report 2009:13, SP Technical Research Institute of Sweden, Borås, Sweden.

[2] Kildegaard C. (1997). Konstruktiv Udformning af Samlinger i Maritime FRP-Sandwich-Konstruktioner. Aalborg Universitetsforlag, Aalborg University, Aalborg, Denmark.

[3] Det Norske Veritas (2005). DNV Rules for Classification of High Speed, Light Craft and Naval Surface Craft, January 2005. Det Norske Veritas, Hövik, Norway.

[4] Zenkert D. (2005). An Introduction to Sandwich Structures (Student Edition), December 2005. Royal Institute of Technology, Stockholm, Sweden.

[5] Steeves C.A. and Fleck N.A. (2004). Collapse Mechanisms of Sandwich Beams With Composite Faces and Foam Core, Loaded in Three-point Bending. Part II. International Journal of Mechanical Sciences, Vol. 46: 585–608.

[6] Toftegaard H. and Lystrup A. (2005). Design and Test of Lightweight Sandwich T-joint for Naval Ships. Composites Part A: Applied Science and Manufacturing, Vol. 36: 1055–1065.

[7] Shenoi R.A. and Violette F.L.M. (1990). A Study of Structural Composite Tee Joints in Small Boats. Journal of Composite Materials, Vol. 24: 644–666.

[8] Berggren et al. (2007). Design of X-joints in Sandwich Structures for Naval Vessels. In Proceedings of the 10th International Symposium on Practical Design of Ships and other Floating Structures (PRADS2007). Houston, Texas, U.S.A.

[9] Kockums AB (2011). Website, CarboClyde datasheet, http://www.kockums.com/en/products-services/commercial-products/carbocat.

[10] Det Norske Veritas (1996). DNV Strength Analysis of Hull Structures in High Speed and Light Craft. Det Norske Veritas, Hövik, Norway.

[11] Rhinoceros (2011). Rhinoceros Nurbs Modelling Software for Windows. Website, http://www.rhino3d.com/.

[12] ANSYS (2011). ANSYS Engineering Simulation Software. Website, http://www.ansys.com/.

[13] Theotokoglou E. and Moan T. (1996). Experimental and Numerical Study of Composite T-Joints. Composite Materials, Vol. 30: 190–209.

[14] Bozhevolnaya E., Thomsen O.T., Kildegaard A. and Skvortsov V. (2003). Local Effects Across Core Junctions in Sandwich Panels. Composites Part B: Engineering, Vol. 34: 509–517.

## Appendix A: Convergence studies

The 2D model convergence study was conducted for a compression test with fixed bottom boundary conditions. This test is shown in principle in Table 6. The development of the max compressive stress in the core material of Panel A was investigated and is shown in Fig. A1. Figure A2 shows the difference in maximum compressive stress compared to the results for the smallest mesh size.

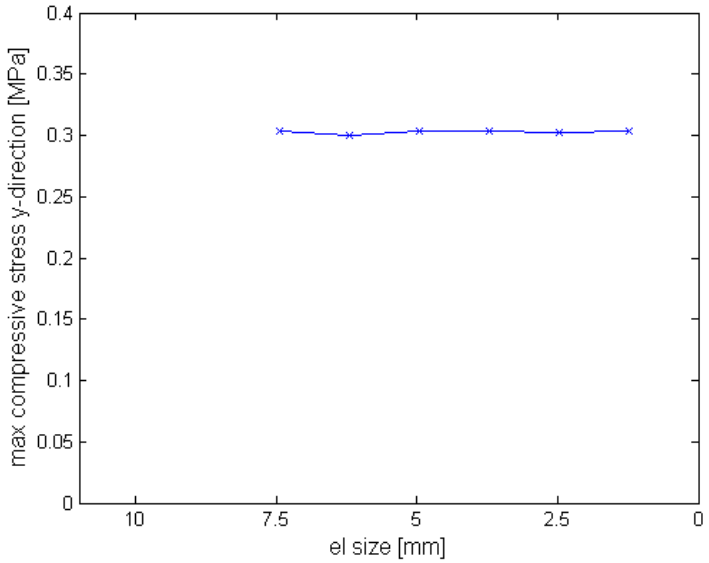


**Fig. A1.** 2D model convergence plot.

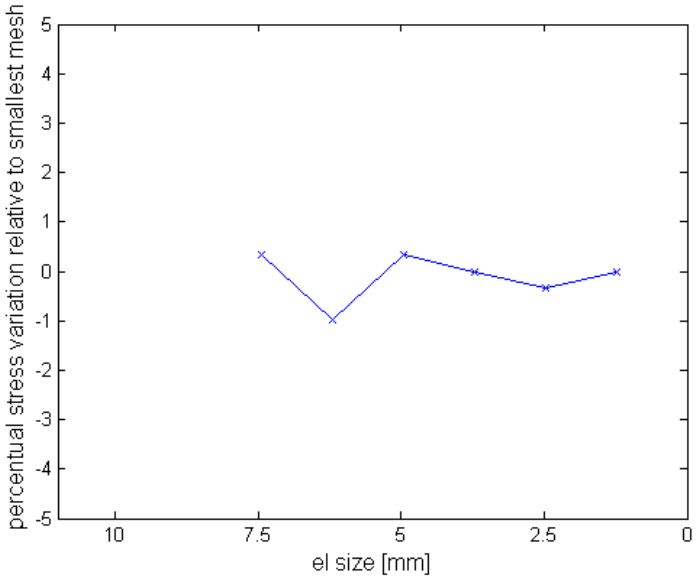


**Fig. A2.** 2D model variation of maximum compressive stress.

The 3D model convergence study was carried out by successively decreasing the element size within the area of interest from element sizes 10, 7.5, 5 down to 4 mm, while keeping the element size outside of the area of interest at 10 mm. Within the area of interest there is a mixed mesh of cubic and pyramid elements and the element size was set by setting the element side length along the lines that define the geometry. For example, in Fig. A5 the

element side length was set on all four boundaries in the x-z plane. The development of the maximum compressive stress in the core material in Panel A, the hull side was investigated and a plot is shown in Fig. A3. As can be seen, the results did not converge but they show relatively small differences between the smaller element sizes and the combination of 4 mm and 10 mm elements was considered to be sufficient for the study. In Fig. A4 the difference in maximum compressive stress compared to the results for the smallest mesh size is plotted.

Tests were attempted with an even smaller element size but did were not successful because of limitations in computational power. Using a 10 mm outer mesh and 2.5 mm detailed mesh resulted in a model with 1.5 million nodes.

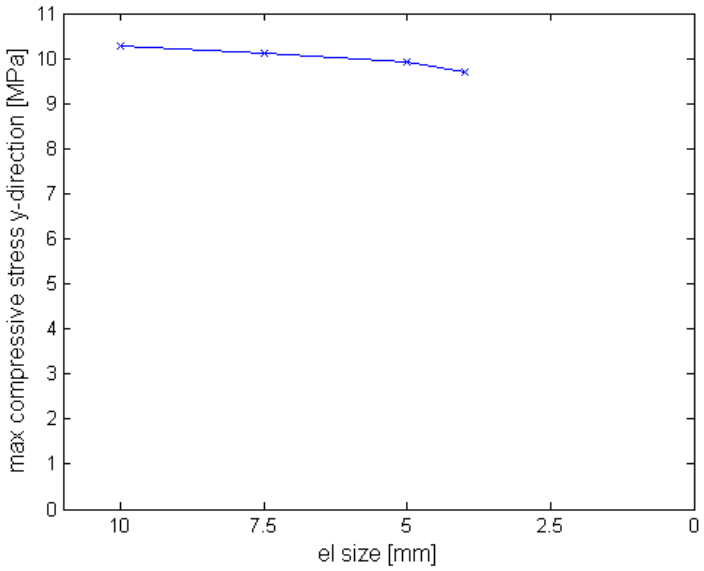


**Fig. A3.** 3D model convergence plot.

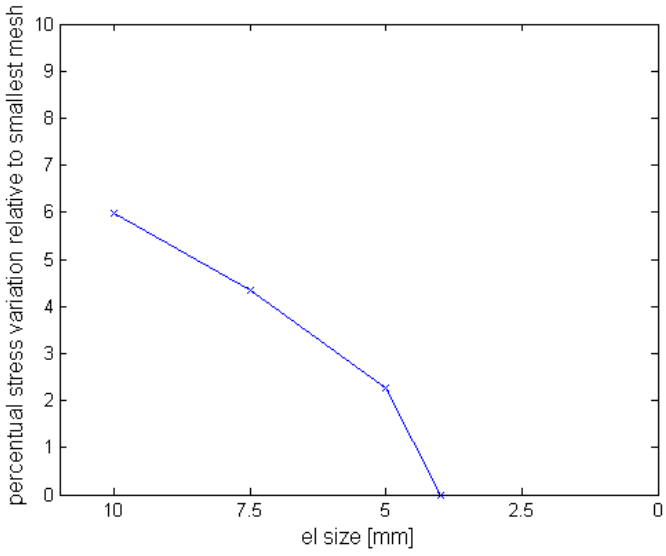


**Fig. A4.** 3D model variation of max compressive stress.

Figure A5 shows the element shape and a plot of the compressive stress distribution at the joint. The element side length is 4 mm.

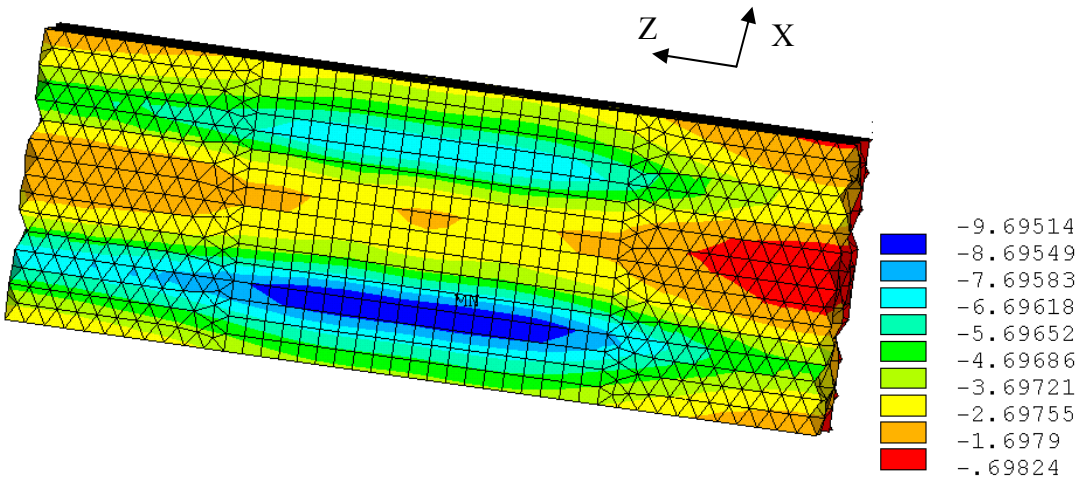


**Fig. A5.** Compressive stress in the y-direction (normal to the paper) of the core material at the joint [MPa].

## Appendix B: 3D joint stress plots for core at intersection point

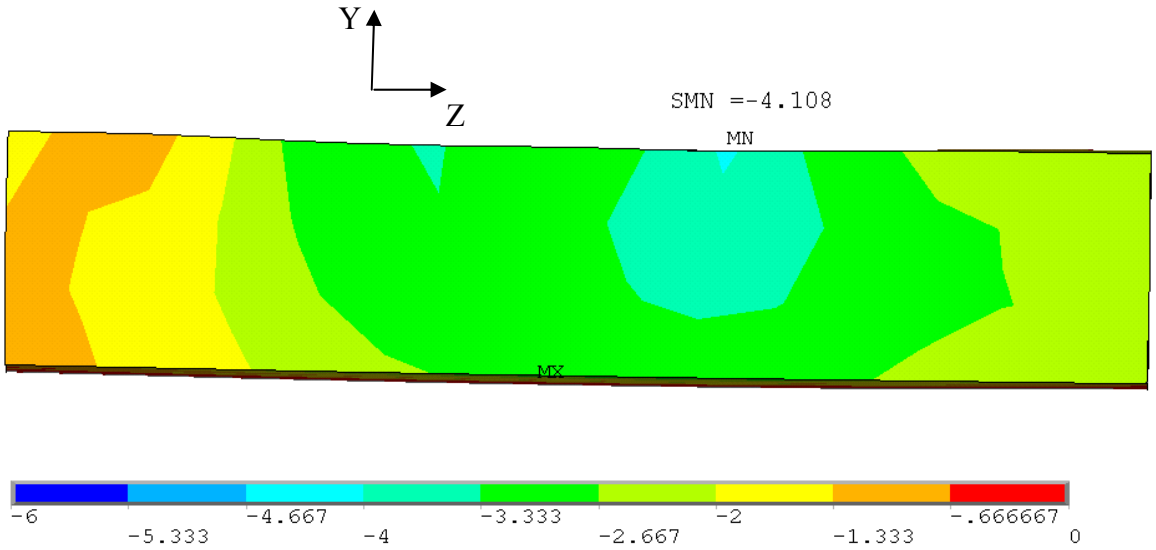


**Fig. B1.** Radius 35 Core H80 compressive stress in the y-direction [MPa].

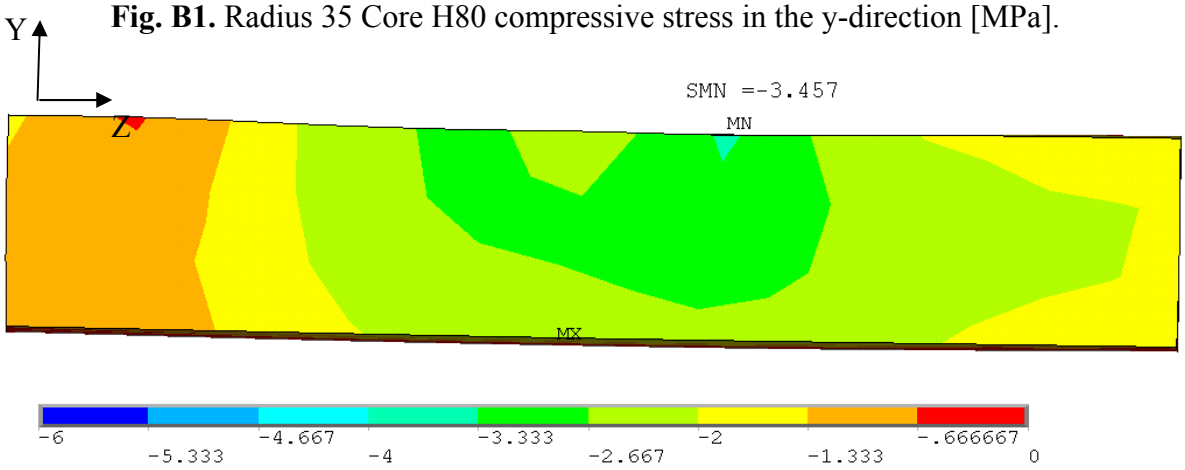


**Fig. B2.** Radius 45 Core H80 compressive stress in the y-direction [MPa].

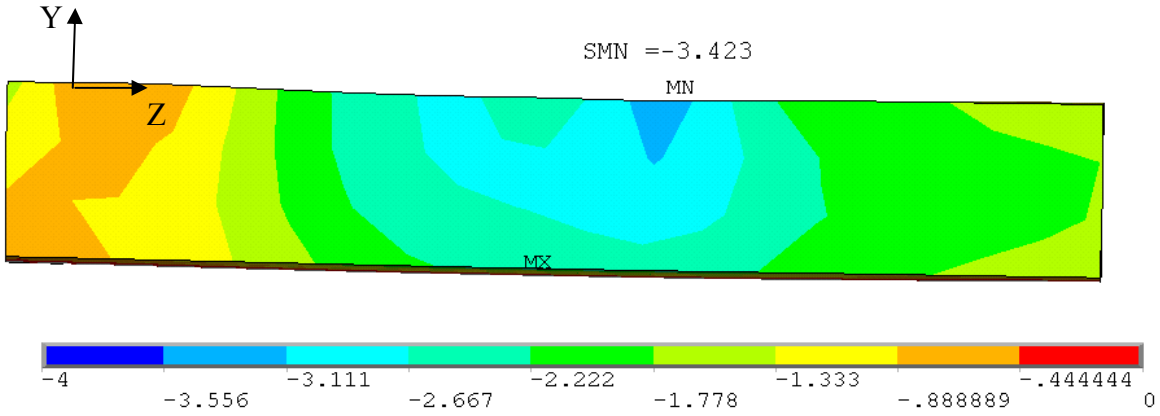


**Fig. B3.** Radius 55 Core H80 compressive stress in the y-direction [MPa].

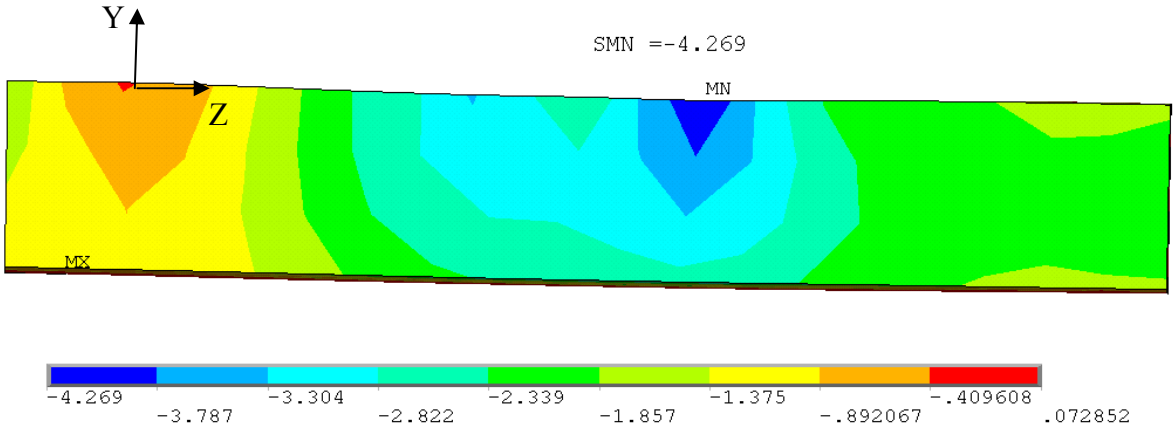


**Fig. B4.** Radius 55 Core H130 compressive stress in the y-direction [MPa].

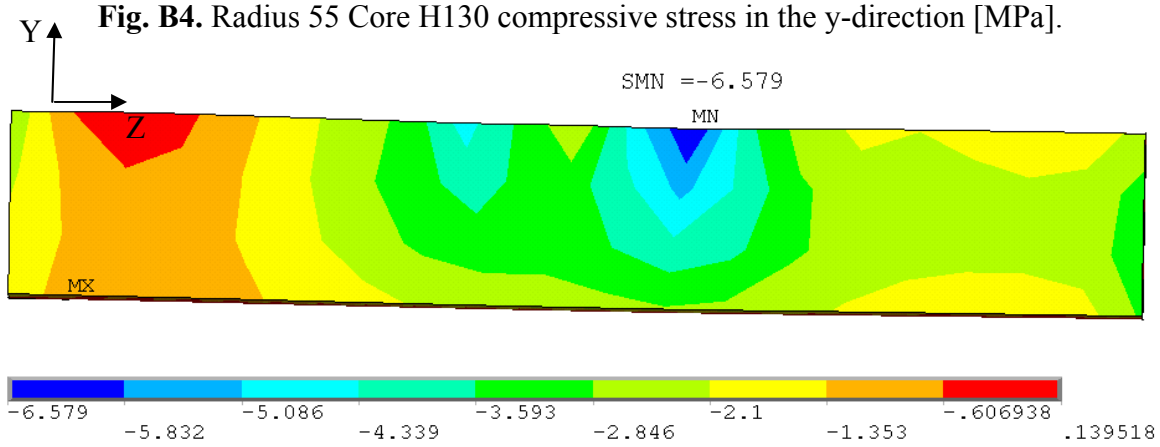


**Fig. B5.** Radius 55 Core H 250 compressive stress in the y-direction [MPa].

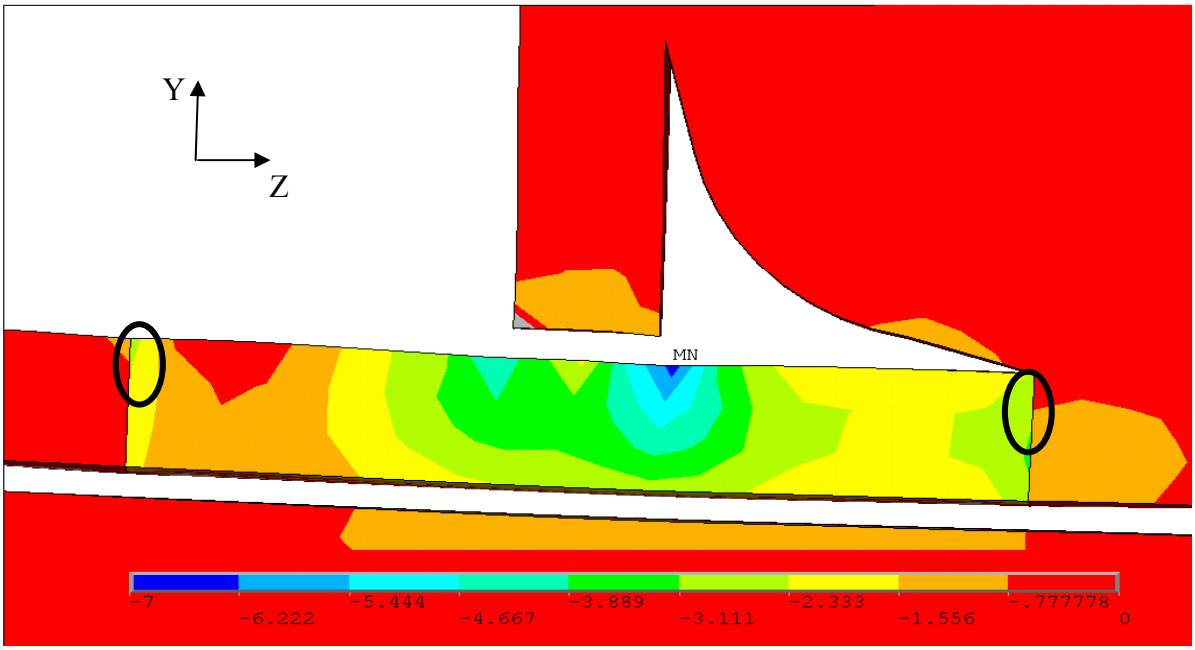


**Fig. B6.** Stress concentrations at H80-H250 compressive stress in the y-direction [MPa].